ELSEVIER

HIGHLIGHTED PAPER

Responsive biomaterials for 3D bioprinting: A review

Zhouquan Fu [1], Liliang Ouyang [2,3,4,*], Runze Xu [2,3,4], Yang Yang [2,3,4], Wei Sun [1,2,3,4,*]

[1] Department of Mechanical Engineering and Mechanics, Drexel University, Philadelphia, PA 19104, USA
[2] Department of Mechanical Engineering, Tsinghua University, Beijing 100084, China
[3] Biomanufacturing and Rapid Forming Technology Key Laboratory of Beijing, Tsinghua University, Beijing 100084, China
[4] "Biomanufacturing and Engineering Living Systems" Innovation International Talents Base (111 Base), Tsinghua University, Beijing 100084, China

Three-dimensional (3D) bioprinting enables a controlled deposition of cells, biomaterials, and biological compounds (i.e., bioinks) to build complex 3D biological models, biological living systems, and therapeutic products. Developing responsive biomaterials as novel bioinks has been a central focus of research in the field of bioprinting because of their controllable material properties in response to printing-induced external or internal stimuli. In this review, we highlight the most recent advances of responsive biomaterials for 3D bioprinting applications. We review commonly used stimuli-responsive biomaterials and strategies for utilizing multifunctional responsiveness to achieve desirable printability, structural formability, cell viability, and construct bioactivity for 3D bioprinting. We also summarize major bioink formulation strategies currently adopted in 3D bioprinting. We subsequently discuss several promising applications of 3D printing involving responsive biomaterials, such as bioprinting in a supporting bath, 4D bioprinting, and bioprinting new controlled drug delivery systems. Future perspectives on the design and development of novel multifunctional bioinks based on responsive biomaterials and technological innovations are also presented.

Keywords: 3D bioprinting; Responsive biomaterials; Bioinks; Printability; Bioactivity

Introduction

Owing to its precise control over the spatial manipulation of cells, biomaterials, and biological compounds [1], 3D bioprinting has attracted tremendous attention in various biomedical applications, including tissue engineering [2–5], disease modeling and etiology [6,7], drug screening [8–10], and personalized medicine [11–14]. A typical paradigm is that a cellularized biomaterial formulation known as bioink is deposited layer-by-layer in a computer-aided manner to fabricate biomimetic tissue constructs. The bioink-related biomaterials, usually in hydrogel form that mimic the extracellular matrix (ECM) of native tissues, not only carry viable cells throughout the deposition process but also provide physical and biochemical signals to regulate cellular activities after fabrication. Thus, formulating biomaterials into favorable bioinks that aid the fabrication and biological processes has been a central focus of interest in the field of bioprinting (see Table 1).

Responsive biomaterials that undergo a physicochemical change in response to internal or external stimuli have been widely used to develop bioinks. Terms including smart [15], intelligent [16], environmental sensitive [17,18], biomimetic [19], and dynamic [20] have been used to describe the responsiveness of these materials. The stimuli can be physical- (e.g., light irradiation, thermal treatment, mechanical stress, electric potential, magnetic field, and water/humidity), chemical- (e.g., pH, nitric oxide, glucose, and redox potential), or biological- (e.g., enzymes, metabolites, and cell traction force) based. The corresponding responses can be physical/chemical crosslinking, bond cleavage, and changes in surface charge, volume, and mor-

* Corresponding authors.
E-mail addresses: Ouyang, L. (ouy@tsinghua.edu.cn), Sun, W. (sunwei@drexel.edu).

 https://doi.org/10.1016/j.mattod.2022.01.001

TABLE 1

Representative responsive biomaterials for 3D bioprinting.

Source	Biomaterials	Responsiveness	Advantages	Disadvantages	Examples
Naturally derived	Alginate	Ionic, pH	• Fast gelation • Low cost	• Poor cell attachment • Slow degradation	[42,56,62,81,82,100,103,113,132,140,150,151,153,156,167,180,197,198]
	Agarose	Thermal	• Gelation at physiological temperature • Mechanically robust	• Poor cell attachment • Excessive water uptake	[43,44,58]
	Chitosan	Ionic, pH	• Antimicrobial • May be osteoconductive	• Poor water solubility • Slow gelation	[45,47,55,61,79,81,83-86,139,158,159,221,229]
	Hyaluronic acid	-	• Interaction with cell surface receptors • Good biocompatibility • Highly accessible for chemical modification	• Requires modification for stable crosslinking	[31,57,59,60,108,121,137,196,228,239]
	Gellan gum	Ionic, thermal	• Rheological modifier and easy to blend with • Mechanically robust	• Poor cell attachment	[49,123]
	Collagen	Thermal, pH	• Major ECM structural protein • Highly bioactive	• Slow gelation • Poor mechanical properties	[50,51,82,83,89-91,110,118]
	Gelatin	Thermal	• Derivative of collagen • Highly bioactive	• Poor mechanical properties	[30,98,107,115,134,136,142,144,159,161,166,213,219,227]
	Fibrin/fibrinogen	Enzyme	• ECM functional protein • Highly bioactive	• Poor long-term stability • Poor mechanical properties	[4,37,52,196]
	Silk fibroin	Enzyme, sonication	• Highly elastic • Good stability	• Poor cell attachment • Might aggregate under shear stress	[40,53,166]
Synthetic	PEG	-	• Chemically well-defined • Allows for versatile chemical modifications • Highly water-soluble	• Poor biodegradability • Poor cell attachment	[31,64,71,109,111,112,131,133,147,218]
	PNIPAAm	Thermal	• Gelation temperature close to 37 °C • Mechanically robust	• Poor biodegradability • Poor cell attachment	[215]
	Poloxamer	Thermal	• Excellent thixotropic properties • Highly water-soluble	• Poor biodegradability • Could be cytotoxic at a high concentration	[57,74,75,243]
	Polyurethane	Thermal	• Good biocompatibility • Tunable sol–gel transition temperature	• Poor biodegradability • Poor cell attachment	[65,213,214,220]

phology [21], all of which would determine the physicochemical and biological properties of formulated bioinks and printed products. Past review articles have generally summarized existing bioinks [22–24] and crosslinking strategies [25,26] for bioprinting, while others have provided a more focused view of physics in bioprinting or specific applications [27–29]. However, there have been many recent advances in bioprinting that emphasize the importance of bioink responsiveness [13,30–34]. Thus, this review will cover state-of-the-art responsive biomaterials for 3D bioprinting applications and highlight the interplay of bioink responsiveness with manufacturing and biological processes.

Here, we consider responsive biomaterials in bioinks that respond to internal and external stimuli before, during, or after extrusion-based bioprinting, the most widely used bioprinting approach. Starting with a brief overview of responsive biomaterials and their composites, we then describe their applications in state-of-the-art 3D bioprinting to design and formulate bioinks, achieving desirable structural printability and biological activities. In particular, we summarize the most recent advances in evaluating and improving bioink printability and cell viability regarding bioink responsiveness, with crosslinking reaction as a significant representative. Various crosslinking mechanisms have been explored to design innovative bioprinting strategies with high structural fidelity and resolution. Strategies that optimize the bioactivity of printed constructs, such as encapsulating bioactive molecules, binding bioactive components to molecular structures, and using decellularized ECM in bioinks are also presented. We then provide a general overview of bioink selection based on different formulations of responsive biomaterials. Finally, we summarize novel applications of responsive biomaterials in supporting baths, 4D bioprinting and drug delivery, together with our perspectives on the future trends in this field. The purpose of this review is to provide a thorough synopsis on bioink development based on responsive biomaterials for bioprinting applications for those who are interested in 3D bioprinting.

General introduction to responsive biomaterials

Responsive biomaterials derived from nature

Naturally derived biomaterials, with biopolymer as a significant representative, can be acquired from animal, plant, and algae sources [35], fermentation of micro-organisms [36], and enzymatic processes [37]. Biopolymers can be grouped into polysaccharides (e.g., alginate, agarose, chitosan, carrageenan, cellulose, gellan gum, pectin, and hyaluronic acid) and proteins (e.g., collagen, gelatin, silk, fibrin, and keratin) based on their chemical composition [38]. Because of the ease of availability and excellent biocompatibility, responsive biopolymers are widely used in biomedical applications [39].

For instance, alginate is a popular linear polysaccharide composed of alternating α-L-guluronic (G unit) and β-D-mannuronic acid (M unit) residues originating from algae and bacteria. Divalent ions (e.g., Ca^{2+}, Mg^{2+}, Ba^{2+}, and Sr^{2+}) can easily crosslink alginate by forming coordination bonds with guluronate blocks [40,41]. The gelation of alginate can also be induced when the pH is below the pKa of G and M units; it involves the combination of decreased alginate solubility, increased unionized carboxyl groups, and water discharge in the formation of gels [42]. Agarose, obtained from red seaweed, is another example of polysaccharide composed of alternating O-3-linked β-D-galactopyranosyl and O-4-linked 3,6-anhydrous-α-L-galactopyranosyl residues [43]. It is thermoresponsive, undergoing reversible gelation at low temperatures. The agarose gel structure comprises double helices with multiple chain aggregation at the junction zone [44]. Chitosan is deacetylated chitin, and its linear chains contain repeating amino monosaccharides similar to glycosaminoglycans (GAGs) [45]. Chitosan hydrogels contain an abundance of cationic amino groups and have low solubility in neutral or basic pH. At pH values below the pKa of chitosan, the amino groups ionize, altering the molecule's electrostatic field, conformation, and solubility. Positive charges along the backbone generate electrostatic repulsion and cause the swelling of chitosan hydrogel [46]. A 1.8% w/w chitosan and 3.6% w/w glycerol phosphate solution is thermoresponsive, and undergoes solution-gelation (sol–gel) transition at 37 °C [47]. Chitosan is also reported to form a hydrogel in response to ions (e.g., tripolyphosphate) and chemical crosslinkers (e.g., glutaraldehyde [48]). Gellan gum, a product secreted by *Sphingomonas elodea* through a fermentation process, is a straight chain of anionic polysaccharides composed of repeating glucose, rhamnose, and glucuronic acid units. Anionic gellan gum can form hydrogel complexes in response to physiological ions (e.g., Ca^{2+}), generating double helices and inter-helical interactions. In addition, the gellan gum solution can form thermoreversible hydrogels when cooling below the sol–gel transition temperature, which makes gellan gum molecules change from a random coil conformation to a double helix [49].

Collagen is an abundant mammalian ECM component and is the most widely used naturally derived biomaterial. Collagen type I can be crosslinked at physiological temperature or neutral pH to form a fibril structure, but this process is usually slow and difficult to control, making it challenging to fabricate [50,51]. Collagen can also be chemically crosslinked using glutaraldehyde, 1-ethyl-(dimethylaminopropyl) carbodiimide (EDC), or enzymes [44]. Gelatin is a hydrolyzed product obtained from either acid- or alkali-treated collagen. An aqueous solution of gelatin can form reversible physical gels via triple helical structure formation upon cooling. Owing to its similar chemical composition to collagen, gelatin can also be crosslinked with similar chemical crosslinking agents. Fibrin is a fibrous ECM protein involved in blood clotting. Fibrin hydrogels are typically formed by the thrombin-mediated polymerization of fibrinogen [4,52]. Silk is a robust natural protein fiber generated by species such as silkworms, spiders, and scorpions. An aqueous solution of silk fibroin from silkworm was reported to undergo a sol–gel transition (crystallization) upon various stimuli, such as shear force, high concentration alcohol solution, high temperature, low pH, electric fields, and sonication [53].

The responsive property of biopolymers can also be introduced by chemical modifications [54–57], such as methacrylation [54], thiolation, and carboxylation [58]. For instance, hyaluronic acid is a glycosaminoglycan (GAG) component widely distributed throughout the body. To form hydrogels, hyaluronic acid usually requires chemical modification to endow stimulus-responsive crosslinking [59]. In the presence of abun-

dant free sites on the backbone (e.g., hydroxyl and carboxyl), hyaluronic acid can be modified with several functional groups such as methacrylates and norbornenes. Methacrylated hyaluronic acid (MeHA) can be photocrosslinked into a hydrogel in the presence of suitable photoinitiator and light [60]. In another example, Ono et al. [61] designed a photocrosslinkable chitosan modified with azide and lactose moieties and used it as an adhesive for soft tissue repair. N_2 is released by the azide group upon UV irradiation, with the reactive nitrene forming azo bond crosslinks. Zheng et al. [62] synthesized ethylenediaminetetraacetic-calcium-alginate (EDTA-Ca^{2+}-Alg) to introduce pH responsiveness. At neutral pH, EDTA-Ca^{2+}-Alg remains in the solution state because EDTA chelates with Ca^{2+}. When the pH is below 4.0, Ca^{2+} is released from EDTA-Ca^{2+} and coordinates with alginate, leading to a sol–gel transition.

Responsive biomaterials based on synthetic polymers

Synthetic polymers can be created by photoelectrically or thermally polymerizing one or more monomers [63–65]. Polyethylene glycol (PEG), poloxamers, poly(N-isopropyl acrylamide) (PNIPAAm), polyvinyl alcohol (PVA), and poly(2-hydroxyethyl methacrylate) (PHEMA) are typical synthetic polymer hydrogels used in bioprinting [66,67]. Synthetic polymers usually possess well-defined chemical structures, molecular weights, and hydrophilicity [68], enabling precise control of their physicochemical properties.

PEG is a hydrophilic polyether widely used in biomedicines as it is highly biocompatible, non-immunogenic, and resists protein absorption [69]. It has been approved by the United States Food and Drug Administration (FDA) for various clinical applications. PEG is available in various structures, such as those with multiple arms. To present responsiveness, PEG can be functionalized with reactive groups such as acrylate [34], thiol [70], and methacrylate [71]. Pluronic F-127 (poloxamer 407) is a commercial product made of poly(ethylene oxide)-b-poly (propylene oxide)-b-poly (ethylene oxide) (PEO–PPO–PEO) triblock copolymers. Pluronic 127 is highly water-soluble and thermoresponsive; at concentrations above 20%, it is aqueous at 4 °C and gelates at 16 °C [72]. Pluronic F-127 has been used to disperse medicines and other molecules throughout the body [73]. It thermo-reversibly gelates and has been used to nucleate vasculature [74] and nanoporous structures [75]. However, it lacks cell-binding domains and might induce cytotoxicity at a high dose, so it is rarely used in tissue engineering applications that require direct contact with living cells [44]. PNIPAAm is a thermoresponsive synthetic polymer with a lower critical solution temperature (LCST) of approximately 32 °C. It undergoes gelation at 32–35 °C and turns into a solution upon cooling [73]. Because PNIPAAm's LCST is slightly lower than physiological temperature, PNIPAAm has been copolymerized with hydrophilic propyl acrylic acid (PAA) [76], acrylic acid (AAc) [77], and methacrylic acid (MAA) [78] to increase LCST. In addition, to modulate the pH responsiveness of PNIPAAm hydrogels [46], some monomers can be introduced, such as anionic monomers (e.g., acrylic acid, and methacrylic acid) and cationic monomers (e.g., dimethylaminoethyl methacrylate, diethylaminoethyl methacrylate, and acrylamide).

Responsive biomaterials based on composite biomaterials

Composite biomaterials refer to combined materials that are either naturally derived or synthetic polymers, or polymers with inorganics or bioactive molecules to achieve specific or multiple responses to environmental stimuli. The main advantage of composite biomaterials is to enable the combination of different properties and overcome the limitations caused by a single component [19]. Specifically, the types of composite combination include natural/natural polymers, natural/synthetic polymers, synthetic/synthetic polymers, polymers/inorganics, and the incorporation of biological factors.

Composite biomaterials have been developed to impart mechanical strength [79,80], bioactivity [81], protein adhesion [82,83], cell affinity [79], and other functionalities [39]. Marsich et al. [81] prepared a new bioactive scaffold from a composite of polyanion (alginate) and a polycation (lactose-modified chitosan), where alginate served as a 3D supporting structure and the modified chitosan mediated the interaction with porcine articular chondrocytes. The composite hydrogel possessed higher mechanical strength and chondrocytes growth promotion than the individual components. The incorporation of natural polymers within synthetic polymers has also been explored extensively. For example, chitosan blended with poly(lactic-co-glycolic acid) [84,85], polyethylene oxide (PEO) [86], and carbon nanotubes [87] has been incorporated into the scaffold to improve its mechanical properties and degradability. Gils et al. [88] synthesized a super-porous hydrogel by free radical graft copolymerization of 2-hydroxyethyl methacrylate (HEMA) and acrylic acid (AA) on xanthan gum (XG). This hydrogel is highly absorbent, biodegradable, and contains few residual monomers. Composite biomaterials incorporated with biological factors are extensively used in drug delivery applications because of their responsiveness to the physiological environment [89–91]. Chem et al. [91] developed a collagen-chondroitin sulfate-based porous scaffold for the controlled release of insulin-like growth factor (IGF-1). IGF-1 was adsorbed to the scaffold through collagen-IGF-1 ionic bonds and the electrostatic attractions between cationic IGF-1 and chondroitin sulfate. The in vitro study showed a burst release of IGF-1 initially and then a steady release for 14 days. Biological molecules can also be incorporated with synthetic polymers to produce conjugated biomaterials [92]. For instance, glucose oxidase and catalase were incorporated into pH-responsive cationic poly(diethylaminomethyl methacrylate-g-ethylene) glycol gels. The activated glucose oxidase converted glucose into gluconic acid, lowered the pH of the environment, and induced sol–gel transitions [93]. Nanomaterials such as gold and SiO2-gold nanoshells have been incorporated into temperature-responsive interpenetrating polymer networks to synthesize thermally responsive nanocomposite systems. The nanoparticles can absorb the heat from environmental light irradiation and transfer it to the polymer networks to produce swelling characteristics [94]. These responsive nanoparticles and

nanocarriers can be developed into multi-stimulus-controlled drug delivery and release systems.

Applying responsive biomaterials to 3D bioprinting

In a typical 3D bioprinting process, biomaterials, living cells, and biological factors are mixed to yield bioinks and then deposited layer-by-layer into a predefined biomimetic 3D construct, during which bioinks undergo physical or chemical crosslinking to stabilize the printed structure [22]. After printing, the cell-laden construct is cultured *in vitro*, where crosslinked bioinks function as ECM to support cell attachment, migration, proliferation, and differentiation, regulated by biomechanical and biochemical cues in the hydrogel microenvironment. Thus, bioinks play a vital role in protecting, delivering, and supporting cells during the bioprinting and subsequent culturing processes. There are some general criteria for bioinks used in extrusion-based bioprinting: (1) bioinks must be extrudable, generate continuous filaments with high fidelity, and form self-supportive hydrogels immediately to keep the printed structure from collapsing [95]; (2) the encapsulated cells in the bioink should remain viable with minimal damage throughout the process; and (3) bioinks used in bioprinting should be biocompatible and supportive to cell growth and tissue maturation [22].

Responsive biomaterials have shown significant potential for bioprinting (Fig. 1). For example, shear-thinning bioinks that respond to shear stress during printing possess good injectability and printability. The decrease in viscosity upon shear stress makes it easier to extrude the bioink, and the viscosity recovery after leaving the nozzle helps maintain filament fidelity. Bioink responses to external or internal stimuli (e.g., ions, pH, light, temperature, and enzymes) that facilitate gelation, can help maintain the shape of a printed construct and provide sufficient mechanical strength for further applications. Additionally, the bioink affects specific and non-specific responses (e.g., strain-stiffening and RGD-mediated binding) to cells that can regulate cell behaviors, such as cell attachment, proliferation, and differentiation, thus endowing the bioink with bioactivities [96,97].

Printability considerations of responsive biomaterials for bioprinting

Characterization of bioink printability

Bioinks with good printability can be dispensed smoothly through the nozzle, form continuous filament with high shape retention, and maintain high structural integrity. Ink composition, viscosity, gelation kinetics, surface tension are typical factors that can affect printability. Extrusion pressure, printing velocity, nozzle diameter, nozzle/printbed/ambient temperature, and printing path are the printing parameters that can affect printing outcome. Whatever parameter configurations are selected, an evaluation approach is needed to characterize the structural outcome, i.e., printability.

There are established methods to evaluate bioink printability through qualitative description [98], quantitative methods [99,100], and computer simulation [101]. Ouyang et al. [99] used a semi-quantitative approach to describe the structural formation of the pore squared by four filaments in a typical lattice design. The ratio of the ideal square circularity (i.e., $\pi/4$) to the actual pore circularity was defined as the printability factor (Pr). A lat-

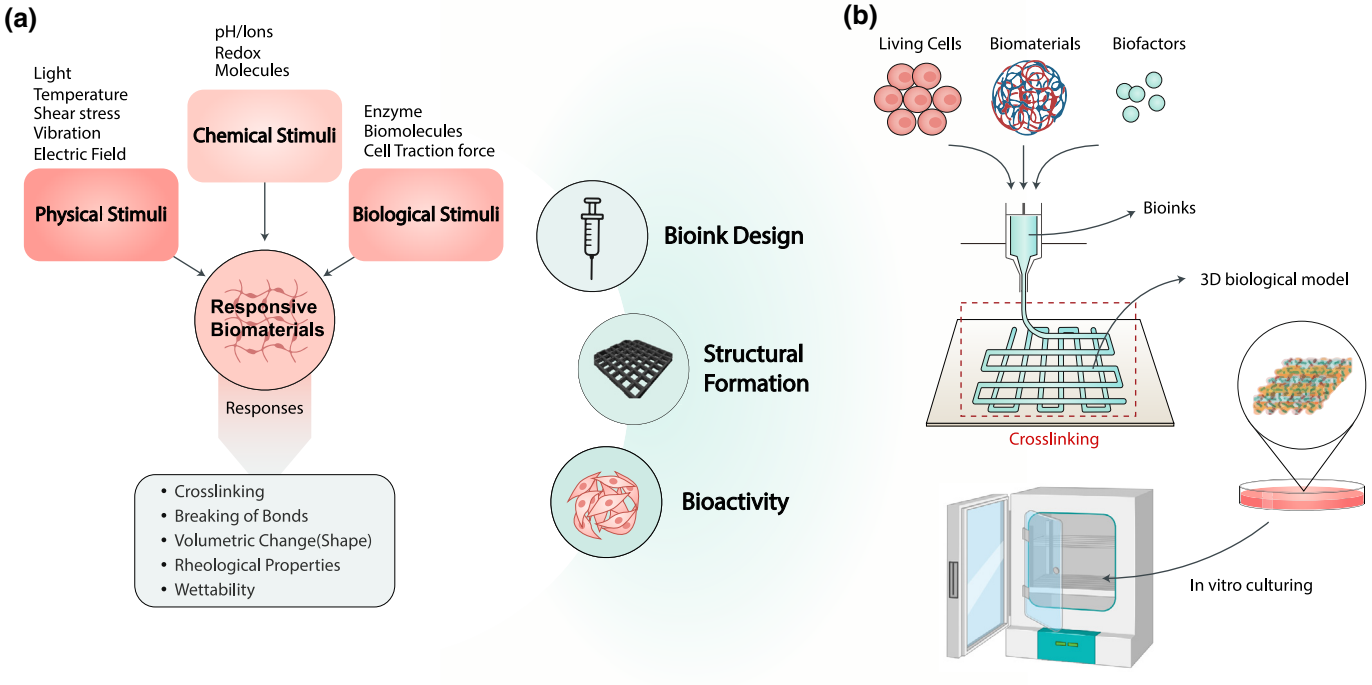

FIGURE 1

Application of responsive biomaterials in 3D bioprinting. (a) Responsive biomaterials can be triggered by physical, chemical, and biological stimuli and respond with crosslinking, breaking of bonds, or changes in shape and wettability. Responsive biomaterials can be used as critical components in bioinks, allowing for structural construction and bioactivity. (b) The general bioprinting process involves the responsiveness of biomaterials from printing to culturing.

tice structure with a Pr value of 1 represents a proper gelation condition, Pr values greater than 1 indicate over-gelation, and Pr values less than 1 represent under-gelation (Fig. 2a). Gohl et al. [101] used a computational tool, IPS IBOFlow (Immersed Boundary Octree Flow Solver), to investigate bioink printability at different viscosities and printer settings. Specifically, a viscoelastic rheology model and surface tension model were used to predict the shape of the printed bioink, which agreed well with the experimental data (Fig. 2b). In another study, bioink printability was evaluated in nanoclay supporting baths with a qualitative method, where the authors observed seven types of filaments – three were identified as well-defined filaments (swelling filament, equivalent diameter filament, and stretched filament) and four as irregular filaments (rough surface filament, over-deposited filament, compressed filament, and discontinuous filament) (Fig. 2c) [102]. Gao et al. [103] introduced a quantitative method to predict printing outcomes and found that the loss tangent (G''/G') correlated with structural integrity and filament uniformity (Fig. 2d). Bioink printability can also be evaluated via rheological properties such as storage and loss moduli [103,104], degree of shear-thinning [105], and yield stress [105,106].

Tailoring printability with bioink properties

Viscosity is a crucial determiner of bioink printability; sufficiently viscous inks can often enhance the printing resolution, shape retention, and stability. However, high viscosity often results in greater shear stress generated within the dispensing nozzle, which might damage embedded cells. Therefore, a tunable bioink viscosity is crucial for good ink printability. For a specific bioink formulation, bioink viscosity varies by temperature [107], shear-thinning properties [108,109], polymer concentration and molecular weight [98,110], encapsulated cell density [111], and the addition of rheology modifying components [112]. Strategies for tuning bioink viscosity are summarized in Table 2. Thermoresponsive biomaterials have temperature-dependent viscosity, which can be exploited for 3D bioprinting via temperature-controlled nozzles [107]. Using a high concentration of biomaterials is a straightforward approach to enhance viscosity, while high polymer density might be toxic to encapsulated cells and limit their access to oxygen and nutrients in the 3D culture system [99]. Polymer molecular weight affects bioink viscosity, depending on the choice of polymer, crosslinker type, and partial crosslinking procedure of bioink precursor [113–115]. The effect of encapsulated cells on bioink viscosity and printing outcome has recently been highlighted [116,117]. It was reported that the viscosity of bioinks can either decrease [99] or increase [118] after encapsulating cells, probably in a cell type and biomaterial-dependent manner. Rheology modifying components are widely used to alter ink viscosity [112,119]. For example, Chen et al. [112] used a high-molecular-weight carbomer colloid as a rheology modifier to improve the 3D printability of acrylamide. Ouyang et al. [30] used gelatin as a universal additive to introduce thermoresponsive rheology to a series of photocrosslinkable hydrogels and achieved standard printability for all the tested bioinks. Shear-thinning behaviors are favorable rheological properties in extrusion-based bioprinting. There are several strategies to introduce shear-thinning properties to bioinks, such as the modifications based on reversible supramolecular and dynamic covalent bonds [40,120,121]. Yield stress is also an important rheological factor associated with ink printability [105,116]. Bioinks behave as a complex fluid if the applied shear stress is higher than the yield stress, initiating the flow of bioinks through the printer nozzle [122]. Once the bioink leaves the nozzle, the applied shear stress is eliminated, and the existing yield stress helps maintain the filament shape [105]. The suitable yield stress of a bioink also prevents sedimentation of cells in the hydrogel precursor and ensures homogeneous cell distribution in the printed tissue [123].

Gelation or crosslinking kinetics of bioinks is another crucial consideration for structural printability. They determine how fast the deposited bioink can crosslink and thus affect the shape fidelity of printed constructs. Slow gelation of bioinks delays crosslinking, and the deposited bioinks spread unfavorably. Furthermore, prolonged gelation time might affect cell viability in the constructs [124] because of the excess exposure to gelation stimuli (e.g., light, temperature, pH, or other harsh conditions). Nevertheless, it is also very important to control the gelation kinetics because rapid crosslinking of bioink in the nozzle can cause an abrupt change of rheological property and clog the dispensing nozzle [106]. Physical crosslinking of biomaterials generates temporary networks stabilized by weak interactions, which include ionic crosslinking, hydrophobic interaction, hydrogen bonds, host–guest interaction, and stereocomplex formation [125]. The mechanically weak and dynamic nature of physical gelation makes it undesirable for use as the only crosslinking mechanism for the solidification of bioprinted constructs. Therefore, physical gelation is often combined with other crosslinking schemes, such as secondary chemical crosslinking [22,106]. Chemical crosslinking introduces covalent bonds in the network, which is likely to improve the mechanical properties and structural fidelity compared with those of physically crosslinked gels. The typical chemistries involved in covalently crosslinked inks include enzyme-mediated crosslinking, photopolymerization (e.g., free radical photopolymerization), and click chemistry (e.g., Michael addition and Schiff base formation).

Surface tension also affects the filament quality and shape fidelity in extrusion bioprinting [126,127]. Bioink surface tension can be influenced by cell density, temperature, and composition [126]. Cell-laden bioinks require adequate surface tension to generate a continuous filament, avoiding droplet formation or attachment to the printing nozzle [128]. Once deposited on the substrate, the bioink filament must maintain a high contact angle with the substrate to retain its shape [129], depending on liquid–gas and liquid–solid surface tensions. In addition, the bioink surface tension and viscoelastic properties counteract possible filament deformation caused by gravity, which helps maintain the structural integrity of the construct [130].

Crosslinking strategies of responsive biomaterials for 3D bioprinting

Bioinks should be instantly crosslinked or stabilized to maintain structural fidelity after being extruded from the nozzle. Responsive bioinks can undergo gelation by applying external or internal stimuli, such as light, temperature, pH, and enzymes before, during, or after extrusion. In the following sections, the

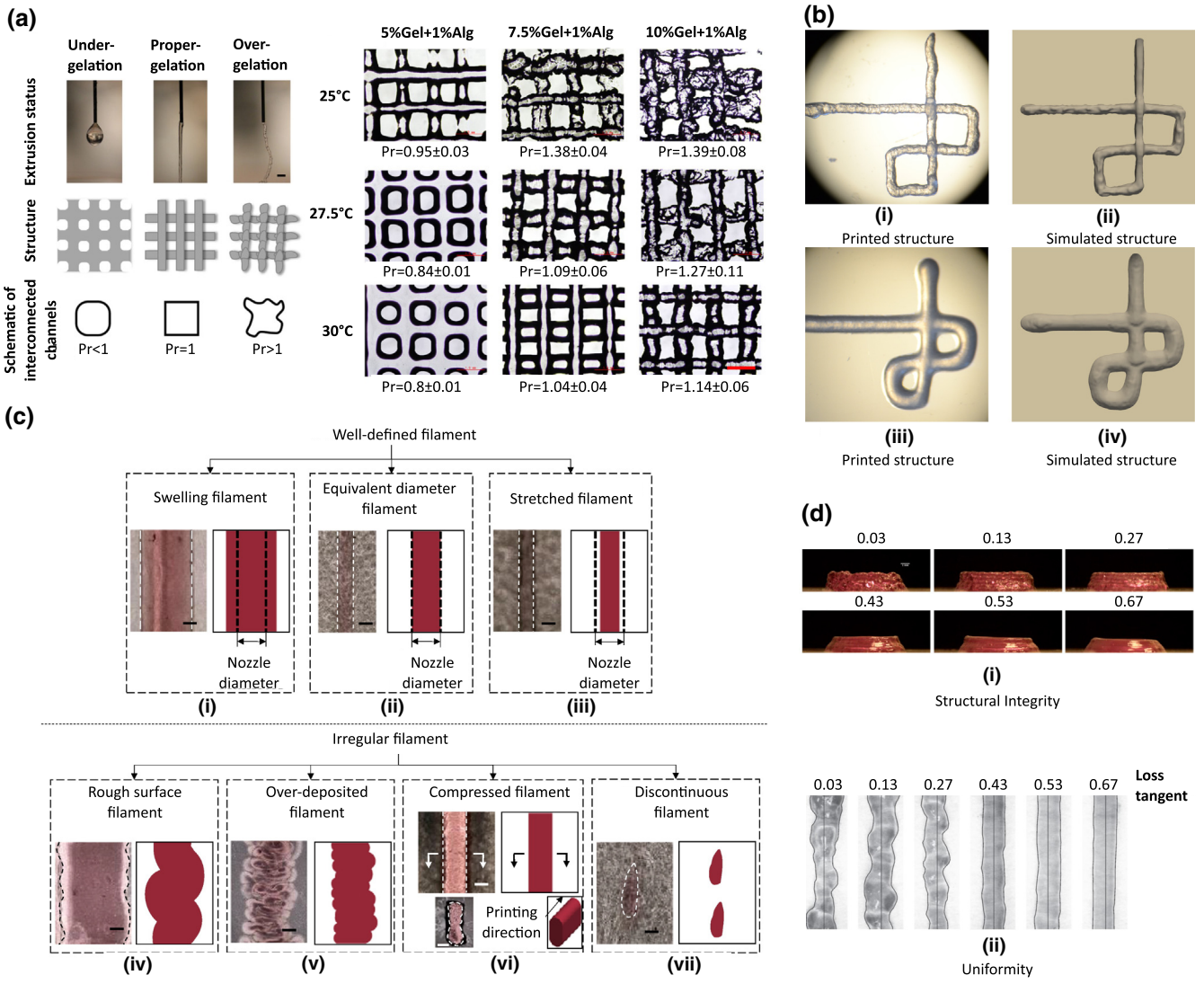

FIGURE 2

Printability determination and characterization. (a) Evaluation of printability under different combinations of gelatin concentration and printing temperature. Printability factor (Pr) was determined based on the convexity of the pore. Filament morphology is presented as under-gelation (Pr < 1), proper-gelation (Pr = 1), and over-gelation (Pr > 1). Reproduced with permission from Ref. [99]. Copyright 2016 IOP Publishing Ltd. (b) (i) Printed grid structure and (ii) the simulation outcome using 4 wt% cellulose nanofibril (CNF) bioink; (iii) Printed grid structure and (iv) the simulation outcome using a CNF-alginate composite bioink. Reproduced with CC BY 3.0 Open Access from Ref. [101]. (c) Filament extrusion uniformity. Seven types of filaments are observed during extrusion in nanoclay supporting bath: (i) swelling filament; (ii) equivalent diameter filament; (iii) stretched filament; (iv) rough surface filament; (v) over-deposited filament; (vi) compressed filament; and (vii) discontinuous filament. Reproduced with permission from Ref. [102]. Copyright 2017 Elsevier B.V. (d) The structural integrity of five-layered structures was evaluated corresponding to different loss tangent values. (i) It was found that loss tangent values of bioink negatively affect the structural integrity. (ii) Filament uniformity of bioinks with different loss tangent values was presented. Proper uniformity was achieved for filaments with loss tangent at 0.43 and higher. Reproduced with permission from Ref. [103]. Copyright 2018 IOP Publishing Ltd.

strategies of utilizing thermo-, photo-, and biochemically responsive materials for 3D bioprinting are discussed in detail (Fig. 3).

Thermoresponsive crosslinking

Thermoresponsive biomaterials have gained much attention because of their tunable temperature-dependent sol–gel transition properties. For biomaterials that possess an LCST, the polymer solution turns increasingly hydrophobic and insoluble upon increasing temperature above LCST, resulting in a gel-like status [73]. While for biomaterials with upper critical solution temperature (UCST), gelation will occur at a temperature below UCST [141]. The ease of sol–gel transition in thermoresponsive biomaterials has made temperature the desired stimulus in the bioprinting process. Commonly used thermoresponsive biomaterials include gelatin, collagen, agarose, chitin, chitosan, cellulose as natural representatives, and PNIPAAm, PEG, and PEO-PPO-PEO (e.g., poloxamers) as synthetic examples [73]. Liu et al. [142] printed gelatin methacryloyl (GelMA) bioink using a cooling process before extrusion. Owing to the formation of the coil-helix structure, GelMA (81.4 ± 4% of methacryloyl substitution) transitioned to a physical gel state at 21 °C and below. By cooling the low-concentration GelMA (3%, 4%, and 5%) at 4 °C for 20 min before deposition at 21 °C, the GelMA

TABLE 2

Representative strategies for tuning printability.

Considerations		Strategies	Advantages	Disadvantages	Examples
Viscoelasticity tuning of bioinks (Rheology)	Temperature	• Thermoresponsive formulations with temperature-dependent viscosity	• Applicable to many commercial printers • Can be achieved by simply mixing with thermoresponsive components	• Requires precise temperature control • Additional/further crosslinking is usually needed	• Gelatin + alginate [107]
	Shear-thinning	• Supramolecular chemistry modification	• Can yield distinct shear-thinning and self-healing properties	• Requires complicated chemical modification • May be difficult to generalize	• Ad-HA + CD-HA [108]
		• Nanoengineered bioink	• Plenty of nanomaterials available • Can introduce additional properties, such as electroconductivity	• Biosafety risk of nanomaterials • Can be difficult for uniform dispersing	• PEGDA + nanosilicates [109]
		• Dynamic covalent chemistry modification	• Can yield reversible bonding • Dynamic bonds can benefit cellular process	• May not be stable enough to maintain structure over time • Requires complicated chemical modification	• HA-HYD + HA-ALD [121]
	Polymer concentration and molecular weight	• Increasing polymer concentration or density	• Convenient for conduction	• Dense polymer network may hinder cell growth	• Alginate + Gelatin [98]
		• Partial crosslinking for increased molecular weight	• Convenient for conduction • Viscosity can be distinctly increased	• Difficult to control the degree of crosslinking • May cause non-smooth extrusion	• Collagen+ GelMA+ tyrosinase [110]
	Cell density	• Embedded cells alter bioink viscosity	• Convenient for conduction	• Effects are dependent on cell type • Optimized cell density may not favor the target tissue formation	• Thiolated HA+ four-arm PEG [111]
	Rheology modifying component	• Rheology modifier	• Convenient for conduction • Easy to generalize	• The added modifier may cause undesired effects on cells • Complete removal of modifier remains challenging	• PEGDA +Carbomer [112]
Gelationmechanism of bioinks	Chemical crosslinking	• Chain growth photopolymerization • Step growth photopolymerization	• Fast gelation kinetics • Remote control of crosslinking • Convenient generalization to plenty of biomaterials	• Risk in cytotoxicity due to the curing light and photoinitiator • May cause depth difference due to light penetration	• Acrylated PCL-PEG-PCL [131] • Alginate-norb+ thiolated crosslinkers [132]
		• Michael-type addition click reaction • Diels–Alder click reaction	• Can be applied to various polymers via chemical modification • Tunable crosslinking degree and mechanical properties	• Continuous crosslinking might result in a short time window for bioprinting	• PEGDA+ PEGDTT [133] • Furan modified gelatin, bismaleimide [134]
		• Schiff-base click reaction			• CMCh+ HAox [135]
		• Enzyme-mediated crosslinking	• Mild reaction condition • No side reaction owing to specificity	• Insufficient crosslinking for multilayered/thick constructs	• HA-Ph, gelatin-Ph with HPR and H2O2 [136]
	Physical crosslinking	• Ionic interaction	• Rapid gelation • Cytocompatible reaction conditions • Can be reversible	• Poor mechanical integrity • Insufficient crosslinking for multilayered/thick constructs	• GelMA+ Gellan gum [123]

(continued on next page)

TABLE 2 (*CONTINUED*)

Considerations	Strategies	Advantages	Disadvantages	Examples
	• Hydrophobic Interaction • Hydrogen bond • Coordination bonds • Host-Guest interaction • Protein–protein interactions	• Can be reversible • Can introduce distinct shear-thinning and self-healing properties	• Poor mechanical integrity • Difficult to define the degree of crosslinking	• Methylcellulose + hyaluronic acid [137] • DNA hybridization [138] • chitosan-catechol+ vanadyl ion [139] • CD-MeHA+ Ad-MeHA [108] • Alginate-peptide+ recombinant protein [98]
Surface tension between bioinks and substrate	• Increase the contact angle between bioink and substrate	• Convenient for conduction • Can be applicable to different bioinks	• May cause discontinuous filament	• Alginate+ Gelatin [140]

PEGDA, poly(ethylene glycol) diacrylate; HA-HYD, hydrazide-modified hyaluronic acid; HA-ALD, aldehyde-modified hyaluronic acid; GelMA, gelatin methacryloyl; PCL, polycaprolactone; Alginate-norb, norbornene functionalized alginate; CMCh, carboxymethyl chitosan; HAox, partially oxidized hyaluronic acid; -Ph, polymers containing phenolic hydroxyl moieties; HPR, horseradish peroxidase; CD-MeHA, methacrylated hyaluronic acid modified with β-cyclodextrin; Ad-MeHA, methacrylated hyaluronic acid modified with adamantane.

physical gel could be smoothly extruded from the nozzle and printed into multi-layered structures without noticeable deformation. Low-concentration GelMA generated a bigger mesh size in the matrix that supported cell survival, proliferation, and migration than its high concentration counterparts. In a recent study [30], 5% gelatin was included in various low-viscosity and low-concentration matrix solutions to introduce thermogelation property suitable for bioprinting. This approach led to breakthroughs in synthesizing low-concentration soft hydrogels constructs favorable for the 3D culture of primary astrocytes.

Reversible thermoresponsive biomaterials could also be used as fugitive materials to template sophisticated structures [74,143,144]. Ouyang et al. [144] developed a void-free bioprinting technique to create 3D vascular channels in thick tissue constructs. In this approach, gelatin and GelMA bioinks were printed side-by-side without voids into multilayers in a temperature-controlled manner. By pre-loading endothelial cells in the gelatin bioink, interconnected endothelialized channels could be generated at 37 °C incubation because of the dissociation of gelatin and *in-situ* seeding of cells. Similarly, Kolesky et al. [74] created 3D bioprinted tissue constructs embedded with vasculatures using Pluronic F127 as fugitive inks. Owing to the nearly opposite thermoresponsivity of Pluronic F127 and GelMA, after photopolymerization of the surrounding GelMA matrix, Pluronic F127 was liquified and removed by cooling the printed construct under 4 °C, forming open channels. The constructs were endothelialized by injecting the HUVEC suspension into the networks; cells were shown to remain 95% viable and form a nearly confluent layer.

Photoresponsive crosslinking

Photoresponsive biomaterials have a significant potential to regulate hydrogel formation spatiotemporally [46]. Photopolymerization could be tuned by varying the light intensity, exposure

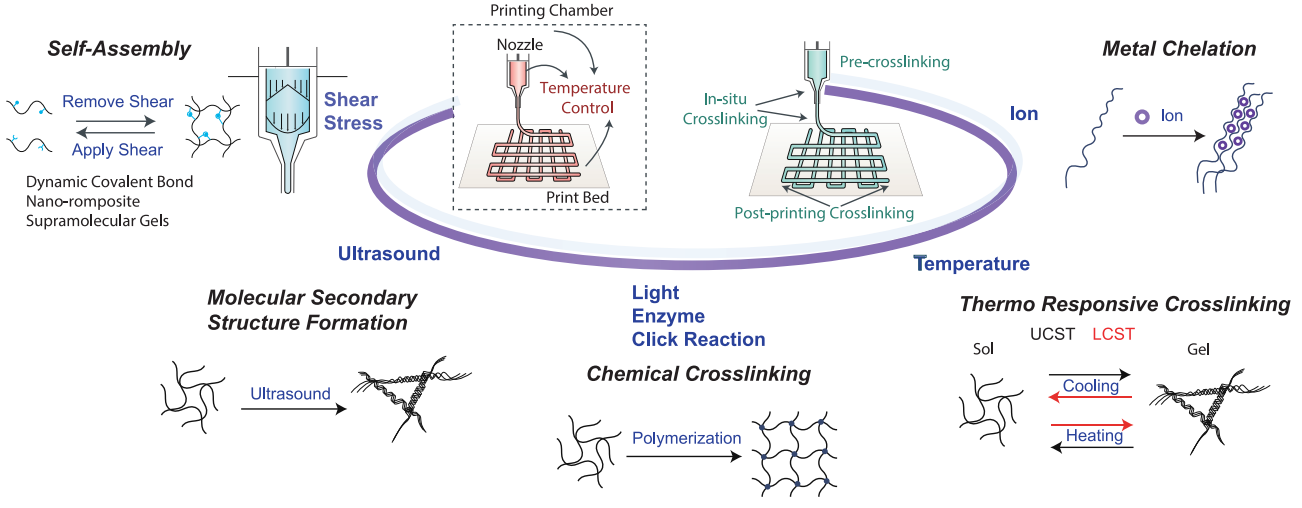

FIGURE 3

Bioink crosslinking mechanisms and application strategies in extrusion-based 3D bioprinting. The stimulus can be applied at the printing chamber, nozzle, or print bed. Crosslinking can take place before, *in-situ*, and after printing.

time, photoinitiator concentration, and photoinitiator efficiency [145]. Common photocrosslinkable biomaterials include those with methacrylate, (di)acrylate, and thiol-ene modifications. For instance, methacrylated polymers can be crosslinked via free radical polymerization in a chain-growth manner. Following light irradiation, the photoinitiator generates free radicals that react with methacrylate groups to crosslink the polymer chains [146]. In contrast, thiol-ene photopolymerization proceeds step-wise, promoting carbon–carbon double bond thiol radical addition and forming crosslinks between complementary reactive groups. Thiol-ene photopolymerization tends to generate more homogenous networks than free radical polymerization [146,147].

Apart from applying light exposure after printing to permanently crosslink the constructs in many studies [22,131,132], light has been introduced prior to [115] or *in-situ* extrusion [31,148] to enhance the printability. For instance, Skardal et al. [115] partially crosslinked bioinks composed of MeHA and gelatin ethanolamide methacrylate by treating with 365 nm UV light for 120 s before printing, producing a printable hydrogel. Then, the printed construct was light-irritated again to obtain a stabilized structure. In another study, Ouyang et al. [31] introduced an *in-situ* photocrosslinking strategy for extrusion-based bioprinting of several nonviscous inks: 2.5 wt% MeHA, 2 wt% norbornene-functionalized hyaluronic acid, 5 wt% PEGDA, and 5 wt% GelMA. By introducing the light to a photopermeable capillary nozzle, all these nonviscous bioinks could be printed into fine filaments and 3D structures, while maintaining high cell viability (~90%).

Biochemical responsive crosslinking

Hydrogels responsive to chemical signals, such as pH and specific ions, have vast applications in controlled drug delivery and regenerative medicine applications [21]. Such chemically responsive biomaterials have also been explored in 3D bioprinting, with collagen, chitosan, keratin alginate, and kappa-carrageenan (κCA) as representatives that respond to pH or ion. Lee et al. [50] recently printed unmodified collagen type I into a human cardiac ventricle, tri-leaflet heart valve, multiscale vasculature, and neonatal-scale human heart with high resolution. Solutions of 12–24 mg/mL collagen were deposited into an optimized supporting bath at pH 7.4, where collagen solidified rapidly. This approach enabled the printing of fine collagen filaments with a diameter down to 20 μm, facilitating the fabrication of anatomically complex structures.

Ionic responsive crosslinking is typically based on the physical crosslink of molecules with opposite electric charges. The ions can form coordination bonds with organic ligands and generate stable gels [149]. Alginate rapidly crosslinks to divalent ions and form a hydrogel upon exposure to Ca^{2+}, Ba^{2+}, and Mg^{2+}. Such favorable gelation properties have led to many novel strategies to use Ca^{2+} as a stimulus in different bioprinting processes. Calcium ions can be applied prior to printing for pre-crosslinking to form cell-laden extrudable bioinks [150]. Ca^{2+} aerosols can also be dispersed using a humidifier over a printed alginate construct to induce alginate gelation [151]. Furthermore, innovative strategies for designing the ion-alginate *in-situ* interactions have been explored, including simultaneous *in-situ* crosslinking of alginate solution with calcium ions from dual nozzles [152], coaxial nozzle [153,154], or deposition of cells with $CaCl_2$ into alginate reservoir [155]. It is worth noting that Ca^{2+} plays an important role in maintaining eukaryotic cellular functionalities (e.g., enzyme activities, metabolic processes, and signal transduction) [156]. At the same time, it can also affect cell survival and proliferation as high ion concentrations will disturb the osmosis balance in the cellular environment [157]. In addition, the electrostatic force between macromolecules can also be utilized to generate a polyelectrolyte complex [158]. Ng et al. [159] used gelatin and chitosan to form polyelectrolyte gelatin-chitosan (PGC) complex hydrogel as acellular bioink in extrusion bioprinting. Gelatin is negatively charged when the pH is above 4.7 (isoelectric point) and will react with the positively charged chitosan and form a hydrogel. The rheological analysis of the PGC hydrogel showed yielding behavior initially and then shear-thinning characteristic with increasing shear rate.

Enzymes incorporated into bioinks to catalyze protein crosslinkage include tyrosinase, transglutaminase, thrombin, and horseradish peroxidase. Tyrosinase was used to facilitate the crosslinking of GelMA and collagen composite bioink [160]. Tyrosine residues in the inks were oxidized by tyrosinase, resulting in pre-crosslinked ink with good printability and mechanical properties. Transglutaminase is a slow-acting calcium-dependent crosslinker that catalyzes glutamyl and lysyl side chain transamination. It has been used in the pre-printing stage to prepare bioinks with excellent shear-thinning properties and thermostability [161]. Thrombin is an enzyme that rapidly transforms soluble fibrinogen into insoluble fibrin [3]. Ning et al. [162] deposited low-viscosity fibrinogen-based bioinks into 10 U/mL thrombin solution to obtain desirably shaped constructs. Horseradish peroxidase (HRP) consumes hydrogen peroxide to catalyze phenyl crosslinking [136]. Sakai et al. [136] prepared a bioink formulation containing polymers with phenolic hydroxyl groups (HA-Ph, gelatin-Ph), HPR, and cells and printed it in an environment with hydrogen peroxide vapor. The extruded inks gelled rapidly to form stable filaments, and the mechanical properties of printed constructs were tunable by controlling HPR and H_2O_2 concentrations.

Other stimuli applied to bioprinting

Other stimuli have also been used to improve cell survivability or assist/initiate the crosslinking process. For example, Koo et al. [163] used a 200 Hz piezoelectric transducer (PZT) to generate microscale vibration to reduce the shear viscosity of bioink, resulting in high cell viability in the printed constructs. Ultrasound (>20 kHz) has been previously reported to align cells in biomaterials for the recapitulation of tissue-specific cell spatial organization [164,165]. It can also be used to initiate the sol–gel physical crosslinking of silk-based biomaterials [40,53]. Das et al. [166] used probe-based sonication during bioprinting to induce gelation of silk fibroin/gelatin-based bioinks. By altering the hydrophobic interaction, sonication can induce conformation of silk fibroin to crystalline antiparallel β-sheet that can self-assemble into a hydrogel. The stiffness of the resultant hydrogel was proved to be higher than that of the enzyme-

mediated crosslinking counterpart. In addition, an electric potential can induce bioink crosslinking *in situ*. Bioinks composed of alginate and $CaCO_3$ crosslinked rapidly after 5 V of potential was applied between the nozzle and print bed. Upon electrostimulation, Ca^{2+} is released from CO_3 and rapidly crosslinks alginate [167].

Biocompatibility considerations of responsive biomaterials for bioprinting

Cell survivability in the bioprinting process

It has been an enduring challenge to achieve both good structural printability and high cell survivability [98,102,168] as some factors that benefit printability negatively affect cell survival [99]. For example, a high viscosity bioink extruded from a nozzle is more likely to yield high filament fidelity and structural integrity [169] but might induce high shear stress and thus cell damage [170]. Particularly, during extrusion, the mechanical driving force generates shear stress within the viscoelastic cell-laden bioinks, resulting in cell damage [171], pyknosis, or karyolysis [172] (Fig. 3a). Chang et al. [170] studied the effect of dispensing pressure and nozzle diameter on cell survival during printing and categorized the cell damage into three types: (1) healthy cells with desirable phenotypes that can proliferate, (2) necrosis and quiescent cells that can either recover or alter to other phenotypes, and (3) apoptosis. It should be noted that, in addition to shear stress, process-induced extensional stress could also cause acute cell death [173,174], where the extrusion flow in the contractive region experiences abrupt velocity changes (Fig. 4b). It was reported that cell-laden alginate ink experienced shear stress-dominated cell damage at dispensing pressures less than 100 kPa, and extensional stress-induced cell damage above 100 kPa [175].

Therefore, bioprinting should occur under mild biomimetic pH and temperature conditions and low shear stress, thus causing minimal damages to the cells. Cell survival during extrusion bioprinting can be affected by bioink properties, printing parameters, and encapsulated cell types. Shear-thinning bioinks, whose viscosity decreases as the shear stress increases during extrusion, are likely to be favorable ink candidates for cells. Bioinks with rapid gelation characteristics are also desired as a prolonged crosslinking process may expose cells to excessive stimuli such as metal ions, pH, or UV light, which can cause unexpected cell damage [124]. Additionally, different bioink compositions will likely affect the rheological properties of bioinks. Therefore, it is imperative to evaluate cell survival rate for different bioink compositions (Fig. 4c) [157]. Printing parameters related to the cell survival include extrusion/print speed [157,176], nozzle diameter [157,170,172], nozzle shape [142,177], and print time [157,178]. Li et al. [157] evaluated the combined effects of motion parameters, nozzle diameter, and printing time on extrusion bioprinting of human induced pluripotent stem cells (hiPSCs) encapsulated in hydroxypropyl chitin based bioink. An ideal parameter region was acquired by intersecting two high viability regions (>90%): one was tested at immediate printing after bioink loading and the other was tested when the printing process was complete (Fig. 4d). In addition, different types of cells have different tolerances to shear stress and requirements for environmental ECM. For example, after printing using the same parameter configuration, nearly 90% of HeLa cells survived; however, only ~14% of embryonic stem cells were alive (Fig. 4e) [99].

Harnessing responsive biomaterials to enhance bioactivity

The bioactivity of bioink is crucial for cell culture and the maturation of bioprinted tissue constructs [24,179,180] as bioactive materials can interact with cells and elicit specific cellular responses [181]. For instance, cell-matrix interactions regulate intracellular signal transduction, which triggers cell physiological responses, such as proliferation, adhesion, migration, and differentiation [182]. Responsive biomaterials can not only provide biochemical cues but also create a dynamic network with tunable stiffness and viscoelastic properties for obtaining the desirable cell activities [183,184]. For example, photocleavage can be used to control the degradation [185] and stiffness of hydrogels [186], and the release of tethered biomolecules or drugs [187]. Electrical responsiveness has also been introduced to hydrogel to control the release of cell-binding peptides [188] and promote signal transmission for neural, muscle, and cardiac tissue engineering [189]. Moreover, thermoresponsive hydrogels have been used to induce changes in the morphology of printed structure, which can affect cellular adhesion [190].

Different methods have been used to enhance the bioactivity, including blending with naturally derived biomaterials and biochemical factors (such as growth factors, cytokines, and proteins), bioconjugation with bioactive motif (such as peptide sequence and growth factor) and use of decellularized ECM bioinks. A typical example is the widely used gelatin-alginate hybrid bioinks, where gelatin or its derivatives are included to introduce cell-binding sites (e.g., arginine-glycine-aspartate peptide, or RGD) that do not exist in plain alginate [191]. Similarly, owing to the poor cell affinity, electrically responsive polymers (e.g., polyelectrolytes) are often incorporated with other biocompatible materials for use in bioprinting. For instance, Spencer et al. [192] developed a conductive composite hydrogel made of GelMA and poly(3,4-ethylenedioxythiophene):poly(styrene sulfonate) (PEDOT:PSS), which possessed tunable swelling, degradation, mechanical properties, and electroconductivity by adjusting the component concentration and ratio. They found out that blending 0.1%(w/v) PEDOT:PSS with GelMA had minimal side effects on the viability and spreading of C2C12 myoblasts compared with using GelMA alone. Additionally, the decrease in impedance of PEDOT: PSS and GelMA composite hydrogel is beneficial for the elongation and differentiation of myoblasts. In their subsequent study, they applied the composite bioink to bioprinting of conductive 3D construct, which showed high cytocompatibility and cell spreading [193]. Matrigel, derived from Engelbreth-Holm-Swarm mouse sarcoma, has excellent bioactivity and has been widely used to formulate bioinks. [7,194]. Li et al. [195] used Matrigel as a bioactive additive in hydroxypropyl chitin inks. They found that increasing the Matrigel concentration in the composite bioink improved the average diameter and variance of hiPSC aggregates, which was critical to further differentiation. As an ECM protein with adhesive peptide sequences [196], fibrin has also been explored extensively as bioink material for stem cell culture and differen-

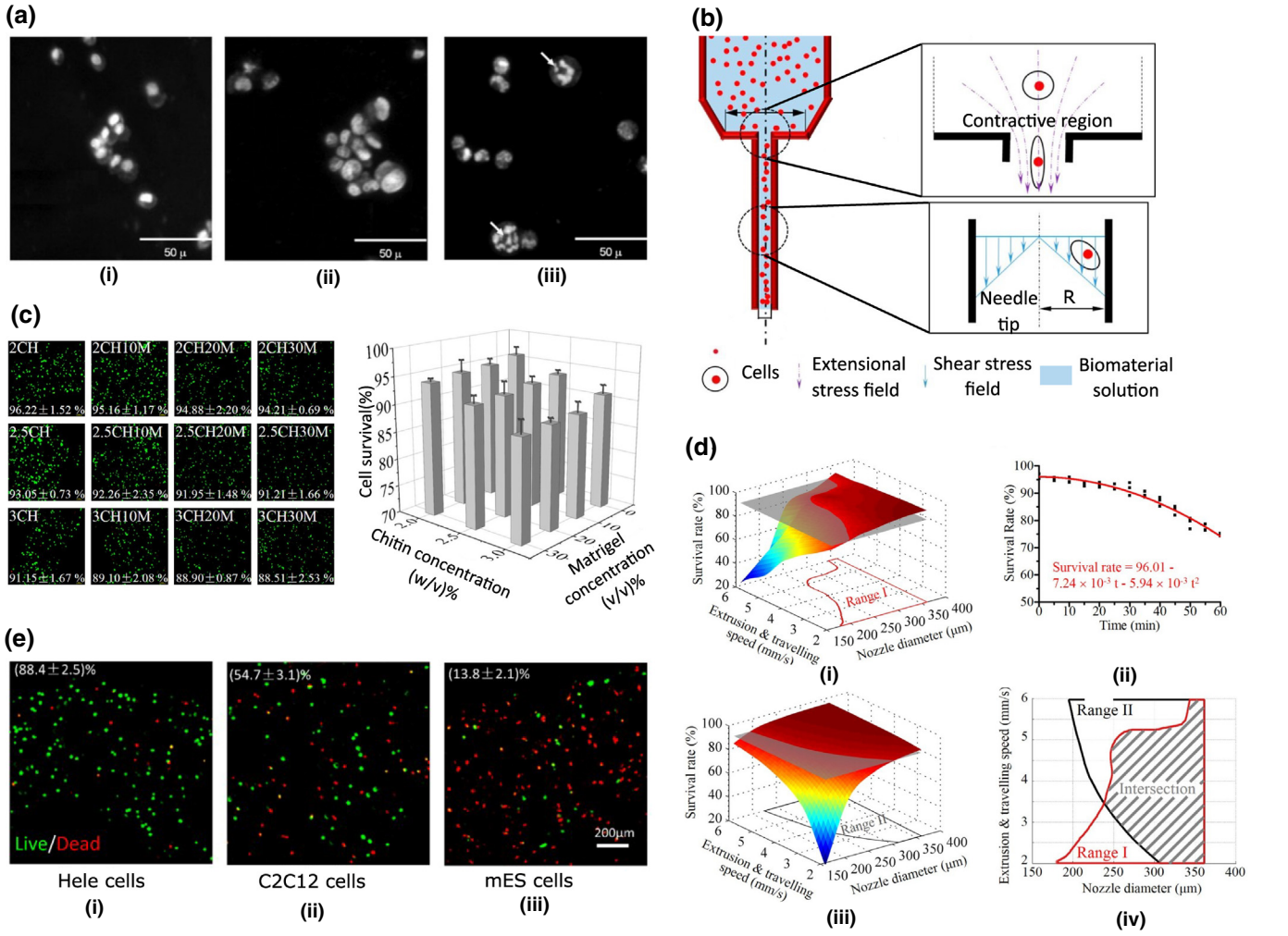

FIGURE 4

Cell survivability during the bioprinting process. (a) Cell morphology (i) before printing, (ii) after printing at 5 psi with 400 mm nozzle, and (iii) after printing at 40 psi with 150 mm nozzle. Reproduced with permission from Ref. [172]. Copy right 2009 WILEY-VCH Verlag GmbH & Co. KGaA, Weinheim. (b) Schematic of process-induced stress distribution inside a needle. Shear stress is developed because of the viscoelastic property of bioink, and extensional stress is generated by the geometrical contractive region between needle and syringe. Reproduced with permission from Ref. [175] Copyright 2018, American Chemical Society. (c) Cell survival rate immediately after bioprinting using bioinks with different hydroxypropyl chitin (CH) and Matrigel ratios. The group 2CH10M referred to the bioink containing 2% (w/v) chitin and 10% (v/v) Matrigel. It was observed that higher bioink concentrations resulted in a lower cell survival rate. The effect of Matrigel concentration on cell survival rate was weaker than that of chitin. Reproduced with permission from Ref. [157]. Copyright 2018 IOP Publishing Ltd. (d) Cell survival rate at different processing parameters. (i) Cell survival rate at different extrusion and travelling speeds and nozzle diameter when the extrusion was initiated. (ii) Cell survival rate plotted with keeping time at 15 °C. (iii) Cell survival rate at different extrusion and traveling speeds and nozzle diameter when the extrusion was completed. A range of parameters was taken where cell viability was maintained to be 90% or above for (i) and (ii). (iv) Intersection of the two ranges represented optimized parameter range to ensure a viability of more than 90%. Reproduced with permission from Ref. [157]. Copyright 2018 IOP Publishing Ltd. (e) Cell survival rate of (i) HeLa cells, (ii) C2C12, and (iii) mouse embryonic stem (mES) cells under the same bioprinting parameters. Reproduced with permission from Ref. [99]. Copyright 2016 IOP Publishing Ltd.

tiation [52]. Abelseth et al. [4] printed hiPSC-derived neural aggregates using fibrin-alginate composite bioinks. On day 41, the early neuronal expression marker class III beta-tubulin was detected, showing that the neural aggregates remained viable and could differentiate in the fibrin-based bioink environment.

Chemical conjugation is also massively used to introduce bioactive motifs to polymers. For example, alginate can be modified with peptides using aqueous carbodiimide chemistry. RGD-conjugated alginate achieves better cell adhesion, viability, proliferation, and ECM expression than unmodified alginate [96]. The alginate polymer backbone can also be partially oxidized into alginate dialdehyde, which can covalently crosslink RGD-containing biomaterials such as gelatin to form a so-called ADA-GEL ink [100,197]. Sarker et al. [198] explored the *in vitro* biocompatibility of ADA-GEL hydrogels and found that the viability, attachment, spreading, and proliferation of fibroblasts increased significantly with ADA-GEL hydrogels than with alginate alone. Growth factors have been conjugated onto 3D printed scaffolds to introduce their bioactive characteristics. Batzaya et al. [199] conjugated vascular endothelial growth factor (VEGF) on GelMA to print vascularized bone tissue. A bioink containing HUVECs, human mesenchymal stem cells (hMSCs), and 5% VEGF-conjugated GelMA with a low degree of methacrylation ($GelMA_{LOW}$-VEGF) was printed into a soft central fiber,

which was later degraded to form perusable vasculature. VEGF-conjugated GelMA (10%) with a high degree of methacrylation ($GelMA_{HIGH}$-VEGF) and containing osteoinductive silicate nanoplatelets and hMSCs was printed around the fiber. By generating a VEGF gradient using the outer $GelMA_{HIGH}$-VEGF layers, enhanced microvasculature formation could be achieved.

Neither natural polymers, synthetic polymers, nor their composites could fully represent the biochemical wealth and complexity of the natural ECM. Advances in research have produced decellularized ECM (dECM) for tissue engineering and regenerative medicine applications [5,13,200,201]. Decellularized ECM from native tissues contains biochemicals from individual compartments, such as fibrous proteins, GAGs, and growth factors [202]. These dECM components create microenvironments that mimic native tissues and modulate cell migration, attachment, proliferation, and differentiation [12]. Meanwhile, dECM is usually thermoresponsive and can form stable hydrogels at physiological salinity, pH, and temperature, which is a promising characteristic for extrusion-based 3D bioprinting [203]. However, collagen-containing dECM hydrogels usually exhibit slow gelation kinetics; hence, various strategies have been implemented to use them as bioinks, including co-printing with supporting structures [204,205], blending with other components [203,206], fabricating dECM into microparticles [13], and optimizing crosslinking strategies [11,202].

Pati et al. [204] developed a method for printing cell-laden dECM bioinks using polycaprolactone (PCL) frameworks. The dECM pre-gels were deposited in the alternating PCL filament gaps for each layer. The constructs remained stable for up to two weeks during *in vitro* culture. In another study, an *in-situ* crosslinking method was applied to print dECM from bovine Achilles tendons bioink. The pre-gel of this bioink was firstly prepared by neutralization with NaOH and PBS. Then a customized printhead aspired the pre-gel into a 37 °C heating unit for 6 min prior to printing. Extruded dECM filaments were intact, and individual fibers were distinguishable from each other, indicating high structural integrity [11]. Other studies have focused on incorporating responsive components or introducing crosslinkers and novel crosslinking mechanisms to dECM hydrogels to increase their printability. Ma et al. [203] developed a photocrosslinkable liver dECM-GelMA ink for projection-based bioprinting.

Overview of bioink formulation strategies

General considerations

Formulating bioinks based on responsive biomaterials follows a set of bioink design criteria, including printability, biocompatibility, bioactivity, and mechanical properties, which have been outlined by several other reviews [179,207–209]. Printability is characterized by extrudability, filament fidelity, and structural integrity [116]. Bioinks empowered by supramolecular chemistry, dynamic covalent chemistry, and nanomaterials often exhibit excellent shear-thinning and self-healing characteristics [120], which are favorable for smooth extrusion through the nozzle. Rapid gelation is also helpful for overall structural integrity. Examples of fast crosslinking mechanisms include photocrosslinking and ionic crosslinking [25]. Multi-responsive bioinks often come in handy as the bioinks can be designed to form shear-thinning gels based on physical or chemical dynamic bonds, then applying a secondary rapid crosslinking to stabilize the printed constructs post extrusion. Bioinks also need to be biocompatible regarding not only the non-toxicity of compositions but also the mild processing conditions for desired cell survival. Naturally derived biomaterials are generally biocompatible and are often blended in composite bioinks. Biodegradability is another important characteristic that can be introduced by functionalizing non-degradable biomaterials with matrix metalloproteinase- or photo-cleavable linkages [210]. Tunable mechanical properties are also essential for tissue-specific applications of bioprinted constructs as different tissues vary in mechanical properties [207]. In the following sections, we will further discuss the strategies available for formulating suitable bioinks using responsive biomaterials.

Single component bioink

Single component bioinks rely on the single component that possesses appropriate rheological and biomimetic properties [211]. Compared to complex bioink compositions and multi-responsive mechanisms, single component bioinks have simpler controllability and fabrication processes, which, on some occasions, can be a better choice for bioprinting. Rhee et al. [51] developed high-density collagen bioinks for extrusion-based bioprinting. They found that heating the deposition plate and formulating inks containing up to 17.5 mg/mL collagen increased the structural fidelity and stability. Cell viability was more than 90% post-printing, indicating that most of the encapsulated cells survived the extrusion of such a high-density collagen bioink.

Functional moieties have been grafted onto biopolymers to improve the mechanical properties and endow them with versatility in printing. Gu et al. [212] printed primary human chondrocytes in a GelMA formulation, which exhibited covalent photocrosslinking with UV light irradiation. Cell viability of 96.13 ± 1.72% was obtained, indicating limited cell injury. However, free radical polymerization of methacrylate groups generates nonbiodegradable backbones and requires low oxygen for efficient crosslinking [132,146]. Ooi et al. [132] developed a norbornene-functionalized alginate bioink crosslinked by thiolated crosslinkers via a thiol-ene reaction to overcome these limitations. This step-growth crosslinking allows for better spatial and temporal control than free radical polymerization. The fast gelation kinetics enabled the use of low-concentration alginate (2 wt%) for better cell viability. In another example, thermoresponsive carboxylated agarose was developed into a mechanically tunable bioink. The elastic modulus of the printed bioink can be tuned by varying the degree of carboxylation while maintaining a similar shear viscosity. Encapsulated hMSCs maintained viabilities of 95%, 91%, and 81% at carboxylation of 28 wt%, 60 wt%, and 93 wt%, respectively [58].

Using responsive synthetic polymers as single-component bioinks has also been explored. Xu et al. [131] developed a triblock copolymer of PCL-PEG-PCL diacrylate, which can be crosslinked in the presence of photoinitiator (lithium phenyl-2,4,6-trimethylbenzoylphosphinate, LAP) and visible light (395–405 nm). The crosslinked hydrogel demonstrated excellent flexibility and elasticity under stretching, compression, and twisting.

After a three-day culture period, 3T3 fibroblasts showed good viability in the hydrogel. Hsiao et al. [213] synthesized a waterborne polyurethane (PU) dispersion with dual-responsive properties from PCL and poly(L-lactide) (PLLA)/poly(D,L-lactide) (PDLLA) diol. The soft segments in the synthesized PUs induce sol–gel transitions near body temperature, the incorporated HEMA endowed the hydrogel with photocrosslinking, and the thermo- and photo-responsiveness of the PUs-HEMA composite bioink significantly improved the ink printability. The PUs promoted cell viability and proliferation after 14 days of culturing when compared with the thermoresponsive control (PUs without HEMA). The growth and differentiation of neural stem cells (NSCs) were also improved in PUs with low modulus (~0.7 kPa) compared with those in a control group (~9 kPa).

Multi-component bioinks

Combining multiple responsive components in ink design intends to integrate the advantages of different bioink compositions [214]. Colosi et al. [191] developed low-viscosity alginate and GelMA composite ink for co-axial extrusion bioprinting. The inclusion of GelMA at a low concentration (<5% w/v) and a low degree of methacryloyl substitution benefits cell organization and encapsulation in 3D, and alginate serves as a structural template owing to its rapid gelation when meeting Ca^{2+}. In another study, Mouser et al. [123] developed a GelMA/gellan gum composite bioink for cartilage bioprinting, where gellan gum significantly mediated the printability and GelMA promoted cartilage-like tissue formation. The study investigated multiple concentrations of GelMA (3–20%) and gellan gum (0–1.5%) and concluded that 10% GelMA and 0.5% gellan gum hybrid formulation is the optimized bioink for cartilage bioprinting with an appropriate stiffness (47.2 ± 4.1 kPa). Thermoresponsive synthetic polymer pNIPAAM was reported to blend with photocrosslinkable MeHA as a versatile bioink in bioprinting. The dual-responsiveness endowed good printability with rapid gelation at 37 °C and the embedded chondrocytes showed 91% viability at day 7 after pNIPAAM was washed away at 4 °C [215].

Biological factors such as growth factors [91], cytokines [216], peptides [217], synthetic crosslinkers [218,219], and proteins [220] have also been incorporated in composite bioinks to tune bioink printability, mechanical property, and biocompatibility. Lin et al. [220] developed a composite polyurethane bioink blended with soy protein. Thermoresponsive PU exhibited sol–gel transition behavior at 37 °C after adjusting the ratio of mixed oligomers (PLLA/PDLLA diol and PCL diol), which is desirable for cell encapsulation and extrusion bioprinting. However, the gelation of the PU dispersion was relatively long, resulting in a narrow time frame for printing. Soy protein is a naturally derived biodegradable thermoplastic polymer that assists the formation of 3D structures. After blending soy protein in PU at a ratio of 1:1.3, the composite bioink possessed a faster gelation time and a wider time frame for bioprinting. In addition, the incorporated NSCs underwent further differentiation and higher oxygen consumption rate, indicating a better microenvironment for NSCs. Crosslinkers could also be incorporated into bioinks to improve their printability and versatility. Rutz et al. [218] presented a composite bioink of amine-containing polymers and PEGX (PEG ending in two reactive groups), a crosslinker based on PEG functionalized with two succinimidyl valerate groups at the ends. PEGX can undergo amine-carboxylic acid coupling with amine-containing gelatin and fibrinogen polymers, resulting in a printable bioink formulation that does not require a high concentration.

Dynamic bioinks

Recent studies on dynamic bioinks have focused on blending interactive components that can self-assemble upon mixing into suitable supramolecular bioinks for bioprinting [60,98,108,138]. Components in these bioinks generate non-covalent bonds and/or supramolecular structures, which induce good printability [98]. Highley et al. [108] used an HA-based supramolecular composite bioink. MeHA was modified with adamantane (Ad, guest) and β-cyclodextrin (CD, host) moieties. Upon blending, Ad-MeHA and CD-MeHA underwent guest–host interactions and formed a supramolecular hydrogel. The supramolecular hydrogel disassembled within the extrusion nozzle because of the generated shear force and self-assembled again after extrusion [60].

Dynamic covalent chemistry can also be applied to design bioinks with shear-thinning properties. Dubbin et al. [98] used two-component hydrogels with complementary peptide-binding domains as bioinks. Alginate was modified with proline-rich peptide domains and an engineered recombinant protein with complementary peptide as the second component. The two components formed into a weak mixing-induced dual-component hydrogel (MITCH) owing to the peptide-peptide interactions. MITCH provided excellent shear-thinning property to protect the encapsulated cells and excellent shape retention for good printability. The characteristics of dynamic covalent bonds can not only endow reversible physical crosslinking but also maintain the bioink robust integrity [40]. Wang et al. [121] modified hyaluronic acid with hydrazide and aldehyde groups to create hydrogel with dynamic hydrazone bonds. The bioinks were extruded with high shape fidelity and structural stability, while encapsulated fibroblasts showed good viability during 14 days of culture. In another example, Liu et al. [221] developed a composite bioink consisting of phenol-functionalized chitosan (Chi-Ph) and dibenzaldehyde-terminated telechelic PEG (DF-PEG). Owing to the dynamic benzoic imine bonds between the amine groups from Chi-Ph and benzaldehyde from DF-PEG, a self-healing hydrogel was formed upon mixing Chi-Ph and DF-PEG at 1:1 ratio. This hydrogel exhibited rapid self-healing ability, which is desired for filament fidelity and construct stackability. Moreover, the hydrogel demonstrated reversible sol–gel transition and behaved as a critical gel (G′ close to G″) under a wide range of strains (360 – 550%), making it highly extrudable.

Nanocomposite bioinks

Nanoengineered composite bioinks incorporate nanoscale components, such as nanofibers, nanotubes, nanoparticles, and other nanomaterials. Adding nanomaterials to inks was reported to induce outstanding shear-thinning characteristics, cell responsiveness, and mechanical properties, which are desirable for 3D bioprinting applications [24,48,222,223]. For example, Markstedt et al. [223] combined nanofibrillated cellulose (NFC) with

alginate to formulate bioinks for cartilage bioprinting. Because of its excellent shear-thinning property, NFC significantly improved the structural fidelity of the composite bioink. An NFC-alginate ratio of 80:20 was optimized to ensure favorable gelling characteristics and high cell viability of human nasoseptal chondrocytes (85.7 ± 1.9% at day 7). In another example, Izadifar et al. [224] engineered a human coronary artery endothelial cell (HCAECs)-encapsulated bioink based on methacrylated collagen (MeCol) and carboxyl-functionalized carbon nanotubes (CNTs). The functionalized CNTs provided a highly connected nanofibrous meshwork that significantly improved viscoelastic properties and electrical conductivity of MeCol. In addition, the encapsulated HCAECs showed high viability (>90%) under optimized UV exposure time and CNT mass ratio after 7 days of culture and exhibited significant proliferation, migration, and differentiation over 10 days of culture.

To improve the mechanical properties of bioprinted constructs, Chimene et al. [225] developed a nanoengineered ionic-covalent entanglement (ICE) bioink, where two-dimensional disk-like Laponite® nanosilicates (nSi) were incorporated into the GelMA/κCA ICE network. In addition to reducing flow resistance during extrusion, the added nanosilicates increased the stability of the ICE network through reversible electrostatic interactions with the charged backbone. They confirmed the strong interaction of GelMA and κCA with nSi by the increased hydrodynamic diameter and stabilized zeta potential. The unique characteristics of nSi can improve the viscoelastic properties and printability of bioinks, showing great potential in bioprinting and tissue engineering applications. Making up 50–70% of bone's dry weight, hydroxyapatite (HAp) is a typical nanomaterial used in bone tissue engineering [222]. Wenz et al. [226] blended GelMA with 40% HAp nanoparticles for 3D printing of human adipose-derived stem cell-encapsulated scaffolds for bone tissue engineering. The incorporation of HAp significantly improved the processibility of GelMA by introducing the shear-thinning property. The mechanical properties were also improved with storage moduli increased from 49.8 ± 1.50 k Pa (pure GelMA of 15 wt%) to 62.2 ± 2.51 kPa and 69.6 ± 1.47 kPa when adding 20% and 40% HAp, respectively.

Frontiers and perspectives

3D bioprinting has evolved from printing biocompatible materials to printing living cell- and organoid-based bioinks for tissue regeneration and personalized medicine [1]. It is a promising technology for fabricating biological models with biomimetic complexity. In the last decade, the demand for structurally complex, high-resolution, and biocompatible bioprints has led to significant efforts in exploring innovative bioinks and bioprinting strategies. This section will briefly introduce the representative frontiers of responsive biomaterials used in bioprinting and provide our perspectives on future trends.

Responsive biomaterials as supporting bath for 3D bioprinting

In addition to being used as building inks, biomaterials with shear-thinning properties are used as supporting mediums for bioprinting conventionally non-printable materials and structures. Bhattacharjee et al. [230] used the granular gel as a supporting medium to support the printing of complex 3D objects with large aspect ratios. The granular gel consisted of 7-μm-diameter Carbopol® microparticles that fluidized at low shear stress for extrusion and resolidified to hold the printed shape. Granular Carpobol® microgels with low yield stress and viscosity filled the trailing crevasse but remained solid at low concentrations. Various hydrogels were printed in the granular gel, including PVA, polyacrylamide, PEG, HA, alginate, and the resulting printed structure had high stability and resolution in the supporting medium. The crosslinked structures were extracted by washing the uncrosslinked Carbopol® gel medium with warm water. In another example, Lee et al. [231] presented a bioprinting method called freeform reversible embedding of suspended hydrogels (FRESH) to fabricate human heart components. FRESH was conducted by depositing collagen into a supporting bath made of a thermoresponsive gelatin microparticle slurry. After the pH-driven crosslinking of extruded collagen, the supporting gelatin medium was removed at 37 °C. In contrast to their previous study, where gelatin microgels were fabricated by blending a solid block of gelatin hydrogels, the authors prepared gelatin particles with a smaller homogeneous diameter and tunable mechanical properties (G' and yield stress) by coacervation. The diameter of the collagen filament printed in the FRESH supporting bath can be as thin as 20 μm, which significantly improved the printing resolution [50]. Noor et al. [232] synthesized a supporting bath composed of alginate microparticles and XG (Fig. 5a). XG is a trisaccharide branched polysaccharide, and its aqueous solution is highly stable and possess shear-thinning property. It could form hydrogen bonding with sodium alginate through the interaction between hydroxyl and carboxyl groups [233]. The resultant supporting medium is transparent and cytocompatible, and the bioprinted constructs could be extracted by aspirating and replacing the bath with alginate lyase containing medium. A thick and cellularized human heart-like tissue model was successfully printed as a proof of concept [227].

Responsive biomaterials for 4D bioprinting

By introducing time as the fourth dimension, 4D bioprinting is believed to have evolved from 3D bioprinting. Because 4D bioprinting is a new paradigm, the definition given by several reviews varies slightly in scope and modalities. An et al. [234] proposed a comprehensive definition that clarifies the three defining components of 4D bioprinting: an automated programmable design, 2D or 3D bioprinting processes, and non-naturally driven transformation that must be triggered externally. The definition excludes processes that are considered natural (e.g., tissue fusion and cell origami induced by cell traction force), which were assumed to be random and not controllable. In another review, Gao et al. [104] defined two 4D bioprinting approaches; one approach involves shape transformation of the responsive biomaterials, and the other approach involves maturation of the printed tissue constructs by cellular coating, self-organization, and matrix deposition. In a more recent review, 4D bioprinting was defined specifically as 3D bioprinting of cell-laden responsive biomaterials with triggers such as intrinsic cell traction forces and external stimulus [235]. Essentially, the resultant 4D printed biomimetic structures obtained by bioprinting stimuli-responsive biomaterials are likely to undergo shape

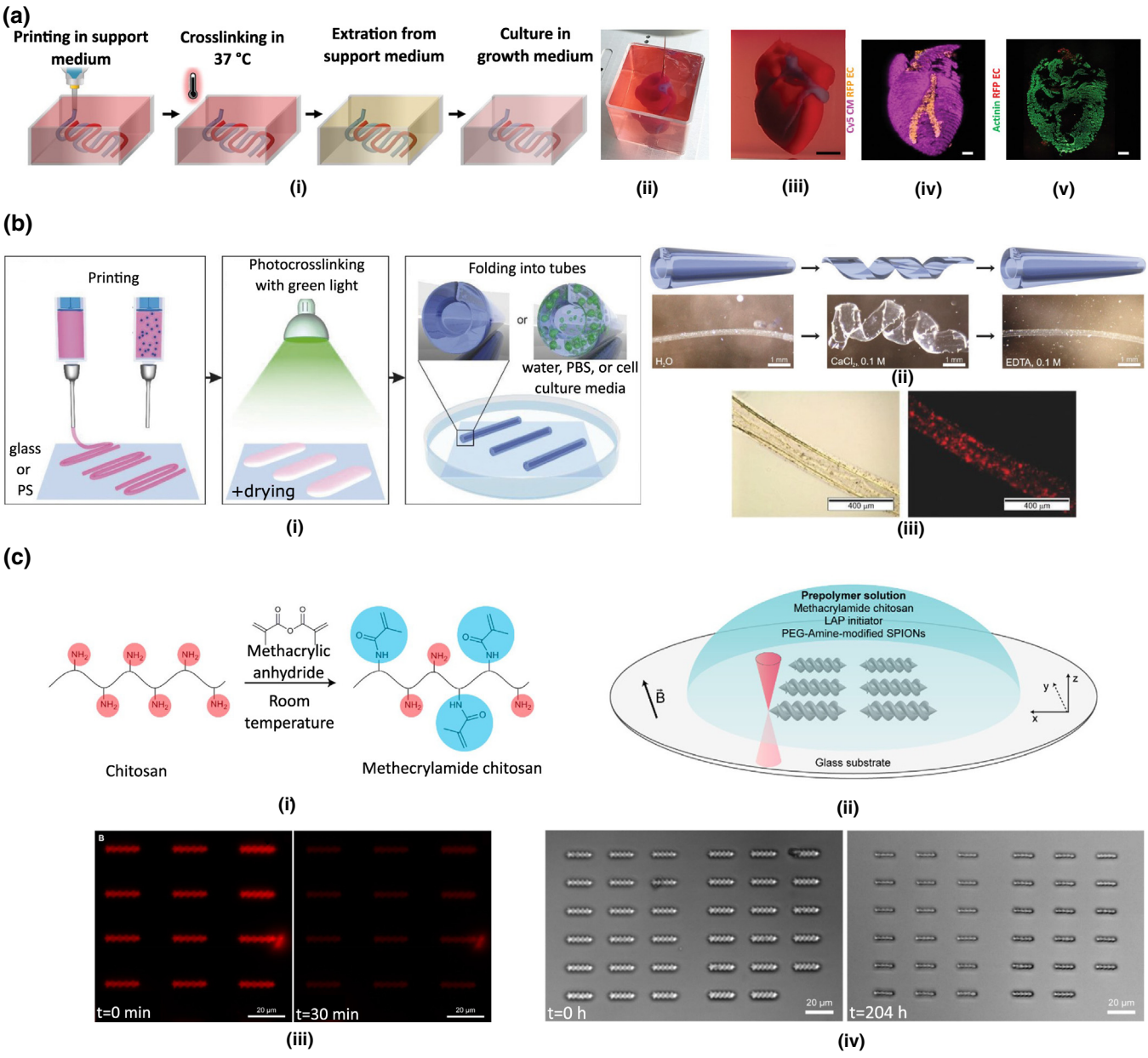

FIGURE 5

Representative applications of responsive biomaterials integrated with 3D bioprinting. (a) 3D bioprinting of thick vascularized heart in supporting bath. (i) Workflow of bioprinting into supporting medium. Designed structure is deposited into a supporting bath composed of alginate microparticles in a xanthan gum-supplemented growth medium. The existence of supporting material allows the crosslinking of dECM-based bioink at 37 °C. The construct can be extracted by aspiration and then moved to a culture medium. (ii, iiii) Thick vascularized heart printed in supporting bath with Cy5-prestained cardiomyocytes (CMs) and RFP-expressing endothelial cells (ECs). Scale bar: 0.5 cm. (iv) Confocal image of printed heart with CMs in pink and ECs in orange. (v) Cross-section image of the printed heart immunostained with sarcomeric actinin. (v, iv) scale bars: 1 mm. Reproduced under CC BY open access license from Ref. [227]. Copyright 2019 Noor et al. Published by WILEY-VCH Verlag GmbH & Co. KGaA, Weinheim. (b) (i) Deposition of methacrylated alginate (AA-MA) and methacrylated hyaluronic acid (HA-MA) with and without mouse bone marrow stromal cells. Exposure of the printed film with 530 nm green light for crosslinking. The construct form into tubes upon immersion into water, PBS, or cell culture media. The top layers in the construct have higher crosslinking density because of more light exposure and thus have a lower swelling ratio than the bottom layers. (ii) AA-MA deformation upon sequentially immersion into water, 0.1 M CaCl2, and 0.1 M EDTA. Ca2+ ions form additional physical bonds with alginate and then can be removed by EDTA (iii) Bright field and fluorescence imaging of the printed cell-laden construct immediately after forming into a tube. Cells were pre-stained with a red fluorescent marker.. Reproduced with permission from Ref. [228]. Copyright 2017 WILEY-VCH Verlag GmbH & Co. KgaA, Weinheim. (c) (i) Synthesis of methecrylamide chitosan. (ii) Fabrication of double helical microswimmer embedding superparamagnetic iron oxide nanoparticles. (iii) Fluorescence image showing the release of doxorubicin (DOX) cleaved from DOX-modified microswimmer by 0.34 w/cm^2 light for 30 min. The fluorescence intensity decreased over a 30 min period. (iv) Microswimmer was treated with lysozyme for 204 h. Optical image showed a surface corrosion-based degradation. Scale bars: 20 μm. Reproduced with permission from Ref. [229]. Copyright 2018, American Chemical Society.

transformation in response to external or internal stimuli. 4D bioprinting technology enables the fabrication of sophisticated tissue constructs as well as on-demand dynamic controls over the shape transformation.

Kirillova et al. [228] developed an approach to fabricate hollow self-folding tubes based on 4D bioprinting of cell-laden responsive biopolymers (Fig. 5b). Cell-laden methacrylated alginate (AA-MA) and MeHA were bioprinted into 2D rectangular shapes on a polystyrene substrate followed by photocrosslinking and mild drying. Owing to the crosslinking gradient in the construct caused by various photoabsorption, the 2D structure swelled and folded into tubes promptly after immersing in an aqueous solution. Biopolymer films formed stable tubes that lasted for at least six months in water without visible degradation. Interestingly, for AA-MA tubes, a reversible folding–unfolding process was achieved by applying Ca^{2+} solutions to induce folding while adding EDTA that chelated Ca^{2+} ions from the alginate-Ca^{2+} network to induce unfolding. The incorporated mouse bone marrow stromal cells (mBMSCs) were homogeneously distributed in the structure with high cell viability after 7 days of culture. More recently, Wu et al. [236] developed a 4D printable bioink composed of gelatin, GelMA, and PU nanoparticles, which can be potentially applied to compact cryopreservation and minimally invasive surgery. The crosslinked composite hydrogel exhibits good shape recovery properties owing to the reversible formation and collapsing of water lattice in the hydrogel network. A ~98% recovery ratio was achieved when immersing the hydrogel constructs in 37 °C water from −20 °C cryopreservation. Moreover, cryopreserved mesenchymal stem cells (MSCs)-laden constructs showed similar proliferation after thawing compared with non-cryopreserved control. In another study, the shape deformation of the bioink was used to increase the resolution of extrusion bioprinting. Gong et al. [237] took advantage of the complexation between positively charged chitosan and negatively charged amino abundant biomaterials (GelMA, MeHA, alginate) to induce shrinking of the construct after bioprinting. The shrink can reduce the size and increase the resolution of printed structures.

Responsive biomaterials as drug delivery vehicle

Stimulus-responsive biomaterials can be used as vehicles to deliver therapeutics because of their inherent ability to communicate with the biological environment. These "smart" biomaterials can respond to biological and pathological signals by mechanisms such as swelling/shrinking, breaking bonds, surface change, and structural change. The controlled drug release of the system is achieved by self-regulation or direct/progressive activation by external or internal stimuli [21,41]. Over the years, traditional 3D printing has been leveraged to fabricate smart drug delivery systems. These responsive biomaterials can be deposited into scaffolds for wound dressings [238], tablets [239,240], and drug-releasing devices [229,241]. Bozuyuk et al. [229] printed a microswimmer device made of methacrylamide chitosan and superparamagnetic iron oxide nanoparticles (Fig. 5c). The ink precursor was fabricated into a double-helix geometry using two-photon direct laser writing. In the presence of a rotating magnetic field, the microswimmer could move at a speed of 3.34 ± 0.71 μm/s. The chemotherapeutic doxorubicin was modified with azide and bonded to the alkyne end of photocleavable molecules. Upon irradiation with 365 nm UV light, the linker molecules were cleaved to release the drug. Furthermore, drug delivery systems can be integrated with bioprinting processes. Examples include the controlled release of growth factors within bioprinted cell-laden constructs for sustained cell functionalities and the transfer of plasmid DNA into cells with temporarily disrupted membranes during extrusion for transfection [8].

Future perspectives

The existing incompatibility between viscous bioinks for high fidelity and cell survival during printing remains to be addressed. Bioprinting of biomimetic heterogeneous constructs with the complexity, mechanical property, and resolution of natural tissues remains a major challenge. We believe there are two paths for future research and development to guide the advancement of bioprinting technology. The first one is the design and formulation of novel responsive biomaterials into suitable bioinks that can be incorporated into the currently available bioprinting techniques. Specifically, bioink development should focus on formulations, crosslinking mechanisms, cytocompatibility and bioactivity. Adopting a composite bioink formulation based on established hydrogel systems may be a convenient strategy for bioink development. Composite bioinks with multi-functional components (e.g., responsive biomaterials, nanoparticles, and crosslinkers) can endow the bioink system with versatility, such as the desired rheological properties for extrusion as well as improved mechanical integrity and biofunctionality of the printed constructs. Meanwhile, the use of novel chemistries to prepare multi-functional responsive hydrogel systems is always an option for developing new bioinks. Considering the dynamic biological process of natural tissue formation, we envision that responsive materials with dynamic viscoelasticity would be attractive for use in 3D bioprinting. The other path is to develop innovative bioprinting strategies that take advantage of the stimulus-responsive properties of biomaterials. Moreover, relevant printability evaluation approaches shall be established towards the standardization of bioprinting outcomes. Machine learning is a powerful tool that may lead to improvement in bioprinting results by optimizing the printing process in many ways, such as adjusting the construct structure, manipulating the printability, and detecting structural defects, considering the difficulty in establishing efficient linkages between bioprinting-associated parameters and resultant physical models in the current paradigm [242,243]. Overall, we envision that biomaterials and bioinks responsive to biological or pathological signals have significant potential in precision medicine, drug delivery, regenerative medicine, and tissue engineering applications.

CRediT authorship contribution statement

Zhouquan Fu: Writing – original draft, Writing – review & editing, Visualization. **Liliang Ouyang:** Conceptualization, Writing – review & editing, Funding acquisition, Supervision. **Runze Xu:** Writing – review & editing. **Yang Yang:** Writing

– review & editing. **Wei Sun:** Conceptualization, Writing – review & editing, Funding acquisition, Supervision.

Declaration of Competing Interest

The authors declare that they have no known competing financial interests or personal relationships that could have appeared to influence the work reported in this paper.

Acknowledgements

This work was supported by Drexel University Sponsored Research Grant (No. 260676), National Natural Science Foundation of China (No. 52105306), Higher Education Discipline Innovation Project (111 Project, No. B17026), and Tsinghua University Faculty Start-up Fund (No. 012-53330200421). The authors acknowledge Cancan Xu for participation in initial discussion and Li Li for the graphical design of Figs. 1 and 3.

Competing interests

The authors declare no competing interests.

References

[1] W. Sun et al., Biofabrication 12 (2) (2020) 022002, https://doi.org/10.1088/1758-5090/ab5158.
[2] P.J. Kondiah et al., Pharmaceutics 12 (2020) 166, https://doi.org/10.3390/pharmaceutics12020166.
[3] H.W. Kang et al., Nat. Biotechnol. 34 (3) (2016) 312–319, https://doi.org/10.1038/nbt.3413.
[4] E. Abelseth et al., ACS Biomater. Sci. Eng. 5 (1) (2019) 234–243, https://doi.org/10.1021/acsbiomaterials.8b01235.
[5] E. Garreta et al., Mater. Today 20 (4) (2017) 166–178, https://doi.org/10.1016/j.mattod.2016.12.005.
[6] X. Ma et al., Adv. Drug Deliv. Rev. 132 (2018) 235–251, https://doi.org/10.1016/j.addr.2018.06.011.
[7] Y. Zhao et al., Biofabrication 6 (3) (2014) 035001, https://doi.org/10.1088/1758-5082/6/3/035001.
[8] W. Peng et al., Acta Biomater. 57 (2017) 26–46, https://doi.org/10.1016/j.actbio.2017.05.025.
[9] H.H. Hwang et al., Biofabrication 13 (2) (2021) 025007, https://doi.org/10.1088/1758-5090/ab89ca.
[10] J. Nie et al., Adv. Healthc. Mater. 9 (7) (2020) 1901773, https://doi.org/10.1002/adhm.201901773.
[11] B. Toprakhisar et al., Macromol. Biosci. 18 (10) (2018) 1800024, https://doi.org/10.1002/mabi.201800024.
[12] S.F. Badylak, D. Taylor, K. Uygun, Annu. Rev. Biomed. Eng. 13 (1) (2011) 27–53, https://doi.org/10.1146/annurev-bioeng-071910-124743.
[13] M.K. Kim et al., Biofabrication 12 (2) (2020) 025003, https://doi.org/10.1088/1758-5090/ab5d80.
[14] H. Yang et al., Gut 70 (3) (2021) 567–574, https://doi.org/10.1136/gutjnl-2019-319960.
[15] F.E. Montero et al., Front. Mech. Eng. 5 (2019), https://doi.org/10.3389/fmech.2019.00056.
[16] J.M. Knipe, N.A. Peppas, Regen. Biomater. 1 (1) (2014) 57–65, https://doi.org/10.1093/rb/rbu006.
[17] Y. Qiu, K. Park, Adv. Drug Deliv. Rev. 64 (2012) 49–60, https://doi.org/10.1016/j.addr.2012.09.024.
[18] A.S. Hoffman, MRS Bull. 16 (9) (1991) 42–46, https://doi.org/10.1557/S0883769400056049.
[19] R.A. Pérez et al., Adv. Drug Deliv. Rev. 65 (4) (2013) 471–496, https://doi.org/10.1016/j.addr.2012.03.009.
[20] J.A. Burdick, W.L. Murphy, Nat. Commun. 3 (2012) 1269, https://doi.org/10.1038/ncomms2271.
[21] Y. Lu et al., Nat. Rev. Mater. 2 (1) (2017), https://doi.org/10.1038/natrevmats.2016.75.
[22] P.S. Gungor-Ozkerim et al., Biomater. Sci. 6 (5) (2018) 915–946.
[23] G. Decante et al., Biofabrication 13 (3) (2021) 032001, https://doi.org/10.1088/1758-5090/abec2c.
[24] D. Chimene, et al. Ann. Biomed. Eng. 44 (2016), 2090-2102, https://doi.org/10.1007/s10439-016-1638-y.
[25] A. GhavamiNejad et al., Small 16 (35) (2020) 2002931, https://doi.org/10.1002/smll.202002931.
[26] N. Ashammakhi et al., Mater. Today Bio 1 (2019) 100008, https://doi.org/10.1016/j.mtbio.2019.100008.
[27] A. Shafiee et al., Phys. Rev. 6 (2) (2019) 021315, https://doi.org/10.1063/1.5087206.
[28] P. Ramiah et al., Front. Mater. Sci. 7 (2020) 76, https://doi.org/10.3389/fmats.2020.00076.
[29] L. Bonetti, L. De Nardo, S. Farè, Tissue Eng. Part B Rev. 27 (5) (2021) 486–513, https://doi.org/10.1089/ten.teb.2020.0202.
[30] L. Ouyang et al., Sci. Adv. 6 (38) (2020), https://doi.org/10.1126/sciadv.abc5529.
[31] L. Ouyang et al., Adv. Mater. 29 (8) (2017) 1604983, https://doi.org/10.1002/adma.201604983.
[32] F.L.C. Morgan, L. Moroni, M.B. Baker, Adv. Healthc. Mater. 9 (15) (2020) 1901798, https://doi.org/10.1002/adhm.201901798.
[33] K. Guo et al., ACS Appl. Mater. Interfaces 13 (2021) 7037–7050, https://doi.org/10.1002/adhm.201901798.
[34] L. Yang, T. Zhang, W. Sun, J. Appl. Polym. Sci. 137 (2020) 49375, https://doi.org/10.1002/app.49375.
[35] O. Murujew, R. Whitton, M. Kube, L. Fan, F. Roddick, B. Jefferson, M. Pidou, Environ. Technol. 42 (10) (2021) 1521–1530, https://doi.org/10.1080/09593330.2019.1673827.
[36] B. Taser et al., Int. J. Biol. Macromol. 183 (2021) 1191–1199, https://doi.org/10.1016/j.ijbiomac.2021.05.062.
[37] B.A. De Melo et al., Acta Biomater. 117 (2020) 60–76, https://doi.org/10.1016/j.actbio.2020.09.024.
[38] M.B. Oliveira, J.F. Mano, Natural-based and stimuli-responsive polymers for tissue engineering and regenerative medicine, in: M.M. Pradas, M.J. Vincent (Eds.), Polymers in regenerative medicine: biomedical applications from nano- to macro-structures, John Wiley & Sons Inc, 2015, pp. 49–90.
[39] W. Zhao et al., J. Chem. Technol. Biotechnol. 88 (3) (2013) 327–339, https://doi.org/10.1002/jctb.3970.
[40] W. Hu, Z. Wang, Y.u. Xiao, S. Zhang, J. Wang, Biomater. Sci. 7 (3) (2019) 843–855.
[41] J.F. Mano, Adv. Eng. Mater. 10 (6) (2008) 515–527, https://doi.org/10.1002/adem.200700355.
[42] C. Hu et al., Int. J. Biol. Macromol. 177 (2021) 578–588, https://doi.org/10.1016/j.ijbiomac.2021.02.086.
[43] M. Tako, S. Nakamura, Carbohydr. Res. 180 (2) (1988) 277–284, https://doi.org/10.1016/0008-6215(88)80084-3.
[44] K.Y. Lee, D.J. Mooney, Chem. Rev. 101 (7) (2001) 1869–1880, https://doi.org/10.1021/cr000108x.
[45] P.S. Bakshi et al., Int. J. Biol. Macromol. 150 (2020) 1072–1083, https://doi.org/10.1016/j.ijbiomac.2019.10.113.
[46] M.C. Koetting et al., Mater. Sci. Eng. R Rep. 93 (2015) 1–49, https://doi.org/10.1016/j.mser.2015.04.001.
[47] E. Ruel-Gariépy et al., Eur. J. Pharm. Biopharm. 57 (1) (2004) 53–63.
[48] N.A. Peppas et al., Adv. Mater. 18 (11) (2006) 1345–1360, https://doi.org/10.1002/adma.200501612.
[49] E.R. Morris, K. Nishinari, M. Rinaudo, Food Hydrocoll. 28 (2) (2012) 373–411, https://doi.org/10.1016/j.foodhyd.2012.01.004.
[50] A. Lee et al., Science 365 (6452) (2019) 482–487.
[51] S. Rhee et al., ACS Biomater. Sci. Eng. 2 (10) (2016) 1800–1805, https://doi.org/10.1021/acsbiomaterials.6b00288.
[52] T.A.E. Ahmed, E.V. Dare, M. Hincke, Tissue Eng. Part B Rev. 14 (2) (2008) 199–215, https://doi.org/10.1089/ten.teb.2007.0435.
[53] S. Chawla et al., Adv. Healthc. Mater. 7 (8) (2018) 1701204, https://doi.org/10.1002/adhm.201701204.
[54] A. Morelli, F. Chiellini, Macromol. Chem. Phys. 211 (7) (2010) 821–832, https://doi.org/10.1002/macp.200900562.
[55] M.H. Cho, et al., Tissue Eng. Part A (2008), 80422095744451, https://doi.org/10.1089/tea.2007.0305.
[56] J.-Y. Wang et al., J. Colloid. Interface Sci. 353 (1) (2011) 61–68, https://doi.org/10.1016/j.jcis.2010.09.034.
[57] H. Lee, T.G. Park, J. Biomed. Mater. Res. 88A (3) (2009) 797–806, https://doi.org/10.1002/jbm.a.31983.
[58] A. Forget et al., Adv. Healthc. Mater. 6 (20) (2017) 1700255, https://doi.org/10.1002/adhm.201700255.
[59] J.A. Burdick, G.D. Prestwich, Adv. Mater. 23 (12) (2011) H41–H56, https://doi.org/10.1002/adma.201003963.

[60] L. Ouyang et al., ACS Biomater. Sci. Eng. 2 (10) (2016) 1743–1751, https://doi.org/10.1021/acsbiomaterials.6b00158.

[61] K. Ono et al., J. Biomed. Mater. Res. 49 (2000) 289–295, https://doi.org/10.1002/(sici)1097-4636(200002)49:2<289::aid-jbm18>3.0.co;2-m.

[62] H. Zheng et al., Carbohydr. Polym. 155 (2017) 329–335, https://doi.org/10.1016/j.carbpol.2016.08.096.

[63] C.N. Medine et al., Stem Cells Transl. Med. 2 (2013) 505–509, https://doi.org/10.5966/sctm.2012-0138.

[64] R.S. Labow, D.J. Erfle, J.P. Santerre, Biomaterials 17 (24) (1996) 2381–2388, https://doi.org/10.1016/S0142-9612(96)00088-9.

[65] F. Khan et al., J. Mater. Chem. B 1 (2013) 2590–2600, https://doi.org/10.1039/c3tb00358b.

[66] M. Caldorera-Moore, N.A. Peppas, Adv. Drug Deliv. Rev. 61 (15) (2009) 1391–1401, https://doi.org/10.1016/j.addr.2009.09.002.

[67] M.L. Bedell et al., Chem. Rev. 120 (19) (2020) 10744–10792, https://doi.org/10.1021/acs.chemrev.9b00834.

[68] A. Skardal, A. Atala, Ann. Biomed. Eng. 43 (3) (2015) 730–746, https://doi.org/10.1007/s10439-014-1207-1.

[69] D.A. Gyles et al., Eur. Polym. J. 88 (2017) 373–392, https://doi.org/10.1016/j.eurpolymj.2017.01.027.

[70] S. Van Belleghem et al., Adv. Funct. Mater. 30 (3) (2020) 1907145, https://doi.org/10.1002/adfm.201907145.

[71] G. Burke et al., J. Mech. Behav. Biomed. Mater. 99 (2019) 1–10, https://doi.org/10.1016/j.jmbbm.2019.07.003.

[72] H. Cui et al., Adv. Healthc. Mater. 6 (1) (2017) 1601118, https://doi.org/10.1002/adhm.201601118.

[73] L. Klouda, Eur. J. Pharm. Biopharm. 97 (2015) 338–349, https://doi.org/10.1016/j.ejpb.2015.05.017.

[74] D.B. Kolesky et al., Adv. Mater. 26 (19) (2014) 3124–3130, https://doi.org/10.1002/adma.201305506.

[75] M. Müller et al., Biofabrication 7 (3) (2015) 035006, https://doi.org/10.1088/1758-5090/7/3/035006.

[76] J.C. Garbern, A.S. Hoffman, P.S. Stayton, Biomacromolecules 11 (7) (2010) 1833–1839, https://doi.org/10.1021/bm100318z.

[77] Y.K. Kim et al., Nanoscale Res. Lett. 14 (2019) 77, https://doi.org/10.1186/s11671-019-2909-y.

[78] J. Wang et al., Mater. Chem. Phys. 239 (2020) 121994, https://doi.org/10.1016/j.matchemphys.2019.121994.

[79] H. Tan et al., Biomaterials 30 (13) (2009) 2499–2506, https://doi.org/10.1016/j.biomaterials.2008.12.080.

[80] V.F. Sechriest et al., J. Biomed. Mater. Res. 49 (2000) 534–541, https://doi.org/10.1002/(SICI)1097-4636(20000315)49:4<534::AID-JBM12>3.0.CO;2-#.

[81] E. Marsich et al., J. Biomed. Mater. Res. 84A (2) (2008) 364–376, https://doi.org/10.1002/jbm.a.31307.

[82] W. Liu, M. Griffith, F. Li, J Mater. Sci. Mater. Med. 19 (11) (2008) 3365–3371, https://doi.org/10.1007/s10856-008-3486-2.

[83] G.R. Ragetly et al., J Mater. Sci. Mater. Med. 21 (8) (2010) 2479–2490, https://doi.org/10.1007/s10856-010-4096-3.

[84] I.K. Shim et al., J. Biomed. Mater. Res. 84A (1) (2008) 247–255, https://doi.org/10.1002/jbm.a.31464.

[85] T. Jiang, W.I. Abdel-Fattah, C.T. Laurencin, Biomaterials 27 (28) (2006) 4894–4903, https://doi.org/10.1016/j.biomaterials.2006.05.025.

[86] Y.-C. Kuo, Y.-R. Hsu, J. Biomed. Mater. Res. 91A (1) (2009) 277–287, https://doi.org/10.1002/jbm.a.32268.

[87] K. Sahithi et al., Int. J. Biol. Macromol. 46 (3) (2010) 281–283, https://doi.org/10.1016/j.ijbiomac.2010.01.006.

[88] P.S. Gils, D. Ray, P.K. Sahoo, Int. J. Biol. Macromol. 45 (4) (2009) 364–371, https://doi.org/10.1016/j.ijbiomac.2009.07.007.

[89] X. Li et al., J. Biomed. Mater. Res. 100A (2) (2012) 396–405, https://doi.org/10.1002/jbm.a.33282.

[90] Y. Wang et al., J. Biomed. Mater. Res. 92A (2010) 693–701, https://doi.org/10.1002/jbm.a.32190.

[91] L.M. Mullen et al., Tissue Eng. Part C Methods 16 (6) (2010) 1439–1448, https://doi.org/10.1089/ten.tec.2009.0806.

[92] E. Gil, S. Hudson, Prog. Polym. Sci 29 (12) (2004) 1173–1222, https://doi.org/10.1016/j.progpolymsci.2004.08.003.

[93] K. Podual, F.J. Doyle, N.A. Peppas, J. Control. Release 67 (1) (2000) 9–17, https://doi.org/10.1016/S0168-3659(00)00195-4.

[94] M. Bikram et al., J. Control. Release 123 (3) (2007) 219–227, https://doi.org/10.1016/j.jconrel.2007.08.013.

[95] L. Ouyang, Study on microextrusion-based 3D bioprinting and bioink crosslinking mechanisms, Springer, Singapore, 2019.

[96] P. Gatenholm, Preparation and Applications of RGD Conjugated Polysaccharide Bioinks with or Without Fibrin for 3D Bioprinting of Human Skin with Novel Printing Head for Use as Model for Testing Cosmetics and for Transplantation, New Delhi Patent (2019).

[97] P. Fisch et al., Adv. Funct. Mater. 31 (16) (2021) 2008261, https://doi.org/10.1002/adfm.202008261.

[98] K. Dubbin et al., Adv. Healthc. Mater. 5 (19) (2016) 2488–2492, https://doi.org/10.1002/adhm.201600636.

[99] L. Ouyang et al., Biofabrication 8 (3) (2016) 035020, https://doi.org/10.1088/1758-5090/8/3/035020.

[100] N. Soltan et al., ACS Biomater. Sci. Eng. 5 (6) (2019) 2976–2987, https://doi.org/10.1021/acsbiomaterials.9b00167.

[101] J. Göhl et al., Biofabrication 10 (3) (2018) 034105, https://doi.org/10.1088/1758-5090/aac872.

[102] Y. Jin, W. Chai, Y. Huang, Mater. Sci. Eng. C. 80 (2017) 313–325, https://doi.org/10.1016/j.msec.2017.05.144.

[103] T. Gao et al., Biofabrication 10 (3) (2018) 034106, https://doi.org/10.1088/1758-5090/aacdc7.

[104] Y. He et al., Sci. Rep. 6 (2016) 29977, https://doi.org/10.1038/srep29977.

[105] N. Paxton et al., Biofabrication 9 (4) (2017) 044107, https://doi.org/10.1088/1758-5090/aa8dd8.

[106] J. Malda et al., Adv. Mater. 25 (36) (2013) 5011–5028, https://doi.org/10.1002/adma.201302042.

[107] J.H.Y. Chung et al., Biomater. Sci. 1 (2013) 763–773, https://doi.org/10.1039/C3BM00012E.

[108] C.B. Highley, C.B. Rodell, J.A. Burdick, Adv. Mater. 27 (34) (2015) 5075–5079, https://doi.org/10.1002/adma.201501234.

[109] C.W. Peak et al., Langmuir 34 (3) (2018) 917–925, https://doi.org/10.1021/acs.langmuir.7b02540.

[110] Y. Shi et al., Biomed. Mater. 13 (3) (2018) 035008, https://doi.org/10.1088/1748-605X/aaa5b6.

[111] A. Skardal, J. Zhang, G.D. Prestwich, Biomaterials 31 (24) (2010) 6173–6181, https://doi.org/10.1016/j.biomaterials.2010.04.045.

[112] Z. Chen et al., Adv. Funct. Mater. 29 (20) (2019) 1900971, https://doi.org/10.1002/adfm.201900971.

[113] A.G. Tabriz et al., Biofabrication 7 (4) (2015) 045012, https://doi.org/10.1088/1758-5090/7/4/045012.

[114] S. Tuladhar, C. Nelson, M.A. Habib. Rheological Analysis of Low Viscosity Hydrogels for 3D Bio-Printing Processes. In International Manufacturing Science and Engineering Conference (vol. 85062, p. V001T03A007). American Society of Mechanical Engineers. https://doi.org/10.1115/MSEC2021-63658.

[115] A. Skardal et al., Tissue Eng. Part A 16 (8) (2010) 2675–2685, https://doi.org/10.1089/ten.tea.2009.0798.

[116] Z. Fu et al., Biofabrication 13 (3) (2021) 033001, https://doi.org/10.1088/1758-5090/abe7ab.

[117] G.J. Gillispie et al., Tissue Eng. Part A 26 (23-24) (2020) 1349–1358.

[118] N. Diamantides et al., Biofabrication 11 (4) (2019) 045016, https://doi.org/10.1088/1758-5090/ab3524.

[119] J. Brindha et al., Mater. Today: Proc. 3 (2016) 3285–3295, https://doi.org/10.1016/j.matpr.2016.10.010.

[120] T. Jungst et al., Chem. Rev. 116 (2016) 1496–1539, https://doi.org/10.1021/acs.chemrev.5b00303.

[121] L.L. Wang et al., J. Biomed. Mater. Res. 106 (2018) 865–875, https://doi.org/10.1002/jbm.a.36323.

[122] S. Varchanis et al., Proc. Natl. Acad. Sci. U.S.A. 117 (23) (2020) 12611–12617, https://doi.org/10.1073/pnas.1922242117.

[123] V.H.M. Mouser et al., Biofabrication 8 (3) (2016) 035003, https://doi.org/10.1088/1758-5090/8/3/035003.

[124] S. Jana, A. Lerman, Biotechnol. Adv. 33 (8) (2015) 1503–1521, https://doi.org/10.1016/j.biotechadv.2015.07.006.

[125] L.J. Min, T.Y.S. Edgar, Z. Zicheng, Y.W. Yee, Biomaterials for bioprinting, in: L. G. Zhang, J.P. Fisher, K.W. Leong (Eds.), 3D Bioprinting and Nanotechnology in Tissue Engineering and Regenerative Medicine, Academic Press, 2015, pp. 129–148.

[126] P. Datta et al., Biotechnol. Adv. 36 (5) (2018) 1481–1504, https://doi.org/10.1016/j.biotechadv.2018.06.003.

[127] X. Cui et al., Adv. Healthc. Mater. 9 (15) (2020) 1901648, https://doi.org/10.1002/adhm.201901648.

[128] M. Hospodiuk et al., Biotechnol. Adv. 35 (2) (2017) 217–239, https://doi.org/10.1016/j.biotechadv.2016.12.006.

[129] C. Mandrycky et al., Biotechnol. Adv. 34 (4) (2016) 422–434, https://doi.org/10.1016/j.biotechadv.2015.12.011.

[130] A. Shafiee, C. Norotte, E. Ghadiri, Bioprinting 8 (2017) 13–21, https://doi.org/10.1016/j.bprint.2017.10.001.
[131] C. Xu et al., ACS Appl. Mater. Interfaces 10 (12) (2018) 9969–9979, https://doi.org/10.1021/acsami.8b01294.
[132] H.W. Ooi et al., Biomacromolecules 19 (8) (2018) 3390–3400, https://doi.org/10.1021/acs.biomac.8b00696.
[133] C.W. Peak et al., Adv. Healthcare Mater. 8 (11) (2019) 1801553, https://doi.org/10.1002/adhm.v8.1110.1002/adhm.201801553.
[134] C. García-Astrain et al., RSC Adv. 4 (2014) 35578–35587, https://doi.org/10.1039/C4RA06122E.
[135] M. Puertas-Bartolomé, et al., Polymers 12 (2020), 1986, https://doi.org/10.3390/polym12091986.
[136] S. Sakai et al., Biofabrication 10 (4) (2018) 045007, https://doi.org/10.1088/1758-5090/aadc9e.
[137] N. Law et al., J. Mech. Behav. Biomed. Mater. 77 (2018) 389–399, https://doi.org/10.1016/j.jmbbm.2017.09.031.
[138] C. Li et al., Angew. Chem. Int. Ed. 54 (13) (2015) 3957–3961, https://doi.org/10.1002/anie.201411383.
[139] D. Lee et al., Biomater. Sci. 6 (5) (2018) 1040–1047.
[140] Q. Li et al., Int. J. Bioprinting 7 (2021). https://doi.org/10.18063/ijb.v7i3.394.
[141] N.A. Peppas et al., Eur. J. Pharm. Biopharm. 50 (2000) 27–46, https://doi.org/10.1016/S0939-6411(00)00090-4.
[142] W. Liu et al., Adv. Healthc. Mater. 6 (12) (2017) 1601451, https://doi.org/10.1002/adhm.201601451.
[143] N. Celikkin, et al. Polymers 10 (2018), 555, https://doi.org/10.3390/polym10050555.
[144] L. Ouyang et al., Adv. Funct. Mater. 30 (1) (2020) 1908349, https://doi.org/10.1002/adfm.201908349.
[145] J.L. Ifkovits, J.A. Burdick, Tissue Eng. 13 (10) (2007) 2369–2385, https://doi.org/10.1089/ten.2007.0093.
[146] R.F. Pereira, P.J. Bártolo, J. Appl. Polym. Sci. 132 (2015) 42458, https://doi.org/10.1002/app.42458.
[147] C.L. McGann et al., Macromol. Biosci. 16 (1) (2016) 129–138, https://doi.org/10.1002/mabi.201500305.
[148] C.D. O'Connell et al., Biofabrication 8 (1) (2016) 015019, https://doi.org/10.1088/1758-5090/8/1/015019.
[149] H. Shabbir, C. Dellago, M.A. Hartmann, Biomimetics 4 (2019) 12, https://doi.org/10.3390/biomimetics4010012.
[150] J. Hazur et al., Biofabrication 12 (4) (2020) 045004, https://doi.org/10.1088/1758-5090/ab98e5.
[151] S. Ahn et al., J. Mater. Chem. 22 (2012) 18735–18740, https://doi.org/10.1039/c2jm33749e.
[152] Y. Liu et al., Rapid Prototyp. J. 22 (6) (2016) 947–955, https://doi.org/10.1108/RPJ-07-2015-0090.
[153] C. Colosi et al., J. Mater. Chem. B 2 (39) (2014) 6779–6791.
[154] W. Lim et al., Polymers 12 (10) (2020) 2377, https://doi.org/10.3390/polym12102377.
[155] T. Xu et al., Biomaterials 34 (1) (2013) 130–139, https://doi.org/10.1016/j.biomaterials.2012.09.035.
[156] N. Cao, X.B. Chen, D.J. Schreyer, ISRN Chem. Eng. 2012 (2012) 1–9, https://doi.org/10.5402/2012/516461.
[157] Y. Li et al., Biofabrication 10 (4) (2018) 044101, https://doi.org/10.1088/1758-5090/aacfc3.
[158] H.V. SIther et al., Carbohydr. Polym. 74 (4) (2008) 813–821, https://doi.org/10.1016/j.carbpol.2008.04.048.
[159] W.L. Ng, W.Y. Yeong, M.W. Naing, Int. J. Biol. Macromol. 2 (2016) 53–62. https://doi.org/10.18063/IJB.2016.01.009.
[160] E. Davoodi et al., Adv. Mater. Technol. 5 (8) (2020) 1901044, https://doi.org/10.1002/admt.201901044.
[161] M. Zhou et al., Biofabrication 11 (2) (2019) 025011, https://doi.org/10.1088/1758-5090/ab063f.
[162] L. Ning et al., J. Mater. Chem. B 7 (29) (2019) 4538–4551, https://doi.org/10.1039/C9TB00669A.
[163] Y. Koo, G. Kim, Biofabrication 8 (2) (2016) 025010, https://doi.org/10.1088/1758-5090/8/2/025010.
[164] P. Chansoria et al., Biofabrication 11 (3) (2019) 035015, https://doi.org/10.1088/1758-5090/ab15cf.
[165] P. Chansoria, R. Shirwaiker, Sci. Rep. 9 (2019) 1–17, https://doi.org/10.1038/s41598-019-50449-w.
[166] S. Das et al., Acta Biomater. 11 (2015) 233–246, https://doi.org/10.1016/j.actbio.2014.09.023.
[167] W. Shang et al., Biofabrication 9 (2) (2017) 025032, https://doi.org/10.1088/1758-5090/aa6ed8.
[168] S. Kyle et al., Adv. Healthc. Mater. 6 (16) (2017) 1700264, https://doi.org/10.1002/adhm.201700264.
[169] A. Ribeiro et al., Biofabrication 10 (1) (2018) 014102, https://doi.org/10.1088/1758-5090/aa90e2.
[170] R. Chang, J. Nam, W. Sun, Tissue Eng. Part A 14 (1) (2008) 41–48, https://doi.org/10.1089/ten.a.2007.0004.
[171] E. Axpe, M.L. Oyen, Int. J. Mol. Sci. 17 (2016) 1976, https://doi.org/10.3390/ijms17121976.
[172] K. Nair et al., Biotechnol. J. 4 (8) (2009) 1168–1177, https://doi.org/10.1002/biot.200900004.
[173] B.A. Aguado, W. Mulyasasmita, J. Su, K.J. Lampe, S.C. Heilshorn, Tissue Eng. Part A 18 (7-8) (2012) 806–815, https://doi.org/10.1089/ten.tea.2011.0391.
[174] S.S. Lee et al., Biomed. Microdevices 11 (5) (2009) 1021–1027, https://doi.org/10.1007/s10544-009-9319-3.
[175] L. Ning et al., ACS Biomater. Sci. Eng. 4 (11) (2018) 3906–3918, https://doi.org/10.1021/acsbiomaterials.8b00714.
[176] J. Emmermacher et al., Biofabrication 12 (2) (2020) 025022, https://doi.org/10.1088/1758-5090/ab7553.
[177] M. Li et al., Biotechnol. Prog. 27 (6) (2011) 1777–1784, https://doi.org/10.1002/btpr.679.
[178] Y. Zhao et al., Biofabrication 7 (4) (2015) 045002, https://doi.org/10.1088/1758-5090/7/4/045002.
[179] A. Parak et al., Drug Discov. Today 24 (1) (2019) 198–205, https://doi.org/10.1016/j.drudis.2018.09.012.
[180] Y. Chen et al., J. Mater. Chem. B 8 (25) (2020) 5500–5514, https://doi.org/10.1039/D0TB00060D.
[181] R. Gupta, A. Kumar, Biomed. Mater. 3 (3) (2008) 034005, https://doi.org/10.1088/1748-6041/3/3/034005.
[182] Y.D. Benoit et al., J. Signal Transduct. 2012 (2012) 1–10, https://doi.org/10.1155/2012/248759.
[183] H.W. Ooi et al., Mater. Horiz. 4 (6) (2017) 1020–1040, https://doi.org/10.1039/C7MH00373K.
[184] A. Gelmi, C.E. Schutt, Adv. Healthc. Mater. 10 (1) (2021) 2001125, https://doi.org/10.1002/adhm.202001125.
[185] A.M. Kloxin et al., Science 324 (5923) (2009) 59–63.
[186] C. Yang et al., Nat. Mater. 13 (6) (2014) 645–652, https://doi.org/10.1038/nmat3889.
[187] K.A. Mosiewicz et al., Nat. Mater. 12 (11) (2013) 1072–1078, https://doi.org/10.1038/nmat3766.
[188] L. Zhang et al., Angew. Chem. Int. Ed. 58 (41) (2019) 14519–14523, https://doi.org/10.1002/anie.201907817.
[189] J. Simon, E. Flahaut, M. Golzio, Materials 12 (2019) 624, https://doi.org/10.3390/ma12040624.
[190] R.H. Kollarigowda, A.S. Mathews, S. Abraham, ACS Appl. Bio Mater. 2 (1) (2019) 277–283, https://doi.org/10.1021/acsabm.8b0059510.1021/acsabm.8b00595.s001.
[191] C. Colosi et al., Adv. Mater. 28 (4) (2016) 677–684, https://doi.org/10.1002/adma.201503310.
[192] A.R. Spencer et al., ACS Biomater. Sci. Eng. 4 (2018) 1558–1567, https://doi.org/10.1021/acsbiomaterials.8b00135.
[193] A.R. Spencer et al., ACS Appl. Mater. Interfaces 11 (34) (2019) 30518–30533, https://doi.org/10.1021/acsami.9b07353.
[194] Y. Pang et al., Biofabrication 10 (2018), https://doi.org/10.1088/1758-5090/aadbde 044102.
[195] S. Tasoglu, U. Demirci, Trends Biotechnol. 31 (1) (2013) 10–19, https://doi.org/10.1016/j.tibtech.2012.10.005.
[196] J. Arulmoli et al., Acta Biomater. 43 (2016) 122–138, https://doi.org/10.1016/j.actbio.2016.07.043.
[197] F. Ruther et al., J. Mater. Sci.: Mater. Med. 30 (2019) 1–14, https://doi.org/10.1007/s10856-018-6205-7.
[198] B. Sarker et al., PLoS One 9 (9) (2014) e107952, https://doi.org/10.1371/journal.pone.0107952.
[199] B. Byambaa et al., Adv. Healthcare Mater. 6 (16) (2017) 1700015, https://doi.org/10.1002/adhm.v6.1610.1002/adhm.201700015.
[200] F. Zhao et al., Acta Biomater. 131 (2021) 262–275, https://doi.org/10.1016/j.actbio.2021.06.026.
[201] S. Chae et al., Biomaterials 267 (2021) 120466, https://doi.org/10.1016/j.biomaterials.2020.120466.
[202] J. Jang et al., Acta Biomater. 33 (2016) 88–95, https://doi.org/10.1016/j.actbio.2016.01.013.
[203] X. Ma et al., Biomaterials 185 (2018) 310–321, https://doi.org/10.1016/j.biomaterials.2018.09.026.

[204] F. Pati, et al., Nat. Commun. 5 (2014), 3935-3935, https://doi.org/10.1038/ncomms4935.
[205] Y. Xu et al., Materials 11 (2018) 1581, https://doi.org/10.3390/ma11091581.
[206] A. Athirasala et al., Biofabrication 10 (2) (2018) 024101, https://doi.org/10.1088/1758-5090/aa9b4e.
[207] S.V. Murphy, A. Atala, Nat. Biotechnol. 32 (2014) 773–785, https://doi.org/10.1038/nbt.2958.
[208] S. Ji, M. Guvendiren, Front. Bioeng. Biotechnol. 5 (2017) 23, https://doi.org/10.3389/fbioe.2017.00023.
[209] J. Gopinathan, I. Noh, Biomater. Res. 22 (2018) 1–15, https://doi.org/10.1186/s40824-018-0122-1.
[210] S. Khetan et al., Nat. Mater. 12 (5) (2013) 458–465, https://doi.org/10.1038/nmat3586.
[211] R.F. Pereira et al., Mater. Horiz. 5 (6) (2018) 1100–1111, https://doi.org/10.1039/C8MH00525G.
[212] Y. Gu et al., J. Biomater. Appl. 33 (5) (2018) 609–618, https://doi.org/10.1177/0885328218805864.
[213] S.-H. Hsiao, S.-H. Hsu, ACS Appl. Mater. Interfaces 10 (35) (2018) 29273–29287, https://doi.org/10.1021/acsami.8b08362.
[214] C.-T. Hsieh, S.-H. Hsu, ACS Appl. Mater. Interfaces 11 (36) (2019) 32746–32757, https://doi.org/10.1021/acsami.9b10784.
[215] M. Kesti et al., Acta Biomater. 11 (2015) 162–172, https://doi.org/10.1016/j.actbio.2014.09.033.
[216] C. Jorgensen, M. Simon, Cells 10 (2021) 596, https://doi.org/10.3390/cells10030596.
[217] C. Cofiño et al., Macromol. Mater. Eng 304 (11) (2019) 1900353, https://doi.org/10.1002/mame.201900353.
[218] A.L. Rutz et al., Adv. Mater. 27 (9) (2015) 1607–1614, https://doi.org/10.1002/adma.201405076.
[219] A. Skardal et al., J. Vis. Exp. e53606 (2016), https://doi.org/10.3791/53606.
[220] H.-H. Lin et al., J. Mater. Chem. B 4 (41) (2016) 6694–6705.
[221] Y. Liu et al., Acta Biomater. 122 (2021) 211–219, https://doi.org/10.1016/j.actbio.2020.12.051.
[222] G. Gao et al., Biotechnol. J. 9 (10) (2014) 1304–1311, https://doi.org/10.1002/biot.201400305.
[223] K. Markstedt et al., Biomacromolecules 16 (5) (2015) 1489–1496, https://doi.org/10.1021/acs.biomac.5b00188.
[224] M. Izadifar et al., Tissue Eng. Part C Methods 24 (2) (2018) 74–88, https://doi.org/10.1089/ten.tec.2017.0346.
[225] D. Chimene et al., ACS Appl. Mater. Interfaces 10 (12) (2018) 9957–9968, https://doi.org/10.1021/acsami.7b19808.
[226] A. Wenz, et al., BioNanoMaterials 17 (2016), 179, https://doi.org/10.1515/bnm-2015-0018.
[227] N. Noor et al., Adv. Sci. 6 (11) (2019) 1900344, https://doi.org/10.1002/advs.201900344.
[228] A. Kirillova et al., Adv. Mater. 29 (46) (2017) 1703443, https://doi.org/10.1002/adma.201703443.
[229] U. Bozuyuk et al., ACS Nano 12 (9) (2018) 9617–9625, https://doi.org/10.1021/acsnano.8b05997.
[230] T. Bhattacharjee, et al., Sci. Adv. 1 (2015), e1500655-e1500655, https://doi.org/10.1126/sciadv.1500655.
[231] T.J. Hinton et al., Sci. Adv. 1 (2015), https://doi.org/10.1126/sciadv.1500758 e1500758.
[232] R. McArdle, R. Hamill, Utilisation of hydrocolloids in processed meat systems, in: P. Kerry, J.F. Kerry (Eds.), Processed Meats, Woodhead Publishing, 2011, pp. 243–269.
[233] T. Pongjanyakul, S. Puttipipatkhachorn, Int. J. Mol. Sci. 331 (1) (2007) 61–71, https://doi.org/10.1016/j.ijpharm.2006.09.011.
[234] J. An, C.K. Chua, V. Mironov, Int. J. Biol. Macromol. 2 (2016) 3–5. https://doi.org/10.18063/IJB.2016.01.003.
[235] N. Ashammakhi et al., Biotechnol. J. 13 (12) (2018) 1800148, https://doi.org/10.1002/biot.201800148.
[236] S.-D. Wu, S.-H. Hsu, Biofabrication 13 (4) (2021) 045029, https://doi.org/10.1088/1758-5090/ac2789.
[237] J. Gong et al., Nat. Commun. 11 (1) (2020), https://doi.org/10.1038/s41467-020-14997-4.
[238] F. Abasalizadeh et al., J Biol Eng 14 (1) (2020), https://doi.org/10.1186/s13036-020-0227-7.
[239] H.P. Si et al., Polymers 11 (2019) 1584, https://doi.org/10.3390/polym11101584.
[240] M.i. Li et al., ACS Appl. Mater. Interfaces 9 (27) (2017) 22160–22175, https://doi.org/10.1021/acsami.7b04428.
[241] E. Bari et al., Pharmaceutics 13 (4) (2021) 515, https://doi.org/10.3390/pharmaceutics13040515.
[242] C. Yu, J. Jiang, Int. J. Bioprinting 6 (2020) 253. https://doi.org/10.18063/ijb.v6i1.253.
[243] Z. Fu, V. Angeline, W. Sun, Int. J. Bioprinting 7 (2021) 434. https://doi.org/10.18063/ijb.v7i4.434.